# SPREAD SPECTRUM MULTIPLE ACCESS IN FIBER OPTIC COMMUNICATION

A thesis submitted
in Partial Fulfilment of the Requirements
for the degree of

MASTER OF TECHNOLOGY

by

SATTIRAJU VENKATESWARA RAO

to the

DEPARTMENT OF ELECTRICAL ENGINEERING

INDIAN INSTITUTE OF TECHNOLOGY, KANPUR

JULY, 1984
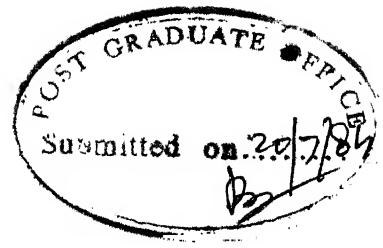
CERTIFICATE

Certified that the work reported in the thesis titled 'SPREAD SPECTRUM MULTIPLE ACCESS IN FIBER OPTIC COMMUNICATION' has been carried out under our supervision by Mr. Sattiraju Venkateswara Rao and has not been submitted elsewhere for a degree.

Dr. K.R. Sarma
Professor
Department of Electrical Engg.
I.I.T.Kanpur
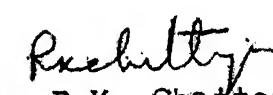
Dr. P.K. Chatterjee
Professor
Department of Electrical Engg
I.I.T. Kanpur
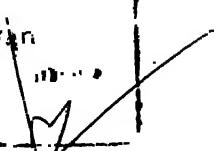
EE-1984-M-RAO-SPR

ABSTRACT

The problem of Multi-user communication with Spread Spectrum Multiple Access over fiber-optic channel has been considered. Specifically Direct Sequence-SSMA situation is considered. Suboptimal receivers, namely, a correlator, and a cascade of inverse filter and a correlator are proposed for this problem in unlimited and limited bandwidth cases respectively. The latter case is introduced at the receiver (not over the channel) in order to reduce the thermal noise effects of the front end circuitry. The performance of the system is evaluated taking into consideration the effect of shot noise. The probability of bit error is evaluated using the Gaussian approximation for the decision statistic. This approach allows us to see the performance dependence on various parameters, like optical power, APD gain, code length of PN sequences, Bias Resistance and number of users etc., more explicitly. The calculated results are presented along with the results of simulation made for the unlimited bandwidth case.

ACKNOWLEDGEMENT

TABLE OF CONTENTS

Page

CHAPTER 1

INTRODUCTION

1.1 THE MULTI-USER COMMUNICATION PROBLEM:

The problem of two or more users communicating over a
single channel has been considered in the past. Such a case
exists in two ways. One is that a group of users is situated
at one end of the channel, and all of them want to communicate
to a similar group of users at the other end of the channel
and vice versa. The second is that the users are geographically
apart and are connected by a network of communication, each
of them wanting to communicate with any other. To achieve this
'Multiplexing' is used in the first case and 'Multiple Access'
in the second case. A vast majority of the existing Multiuser
communication systems use 'Frequency division Multiplexing'
(FDM) or 'Time Division Multiplexing' (TDM) for the first
case and 'Frequency Division Multiple Access' (FDMA) or the
'Time Division Multiple Access' (TDMA) for the second case.

Though known for quite some time the third method
'Spread Spectrum Multiplexing (SSM) or 'Multiple Access' (SSMA),
is being considered as a viable alternative to the above
methods during recent times. Unlike the other two methods
SS Modulation offers some additional advantages in addition
to providing multiplexing or multiple access capability. In

fact these advantages only motivate us to consider SSM(A) instead of TDM(A) or FDM(A). The advantages are narrowband interference rejection, tone frequency (ac or dc) rejection, antijamming capability, and antimultipath capability [1]. It also offers a certain amount of secrecy. Some of these, we show more analytically in Chapter 3. As a multiple access method SS modulation offers an important feature, namely that of asynchronous multiplexing of the users' signals. That is in a network users can be added or dropped with out affecting the performance of the other users. Thus it obviates the need of expensive loop synchronization as in the case of TDMA. Though this feature of asynchronous mode of operation is present in FDMA also, there the use of the channel bandwidth by a particular user is permanately limited to a portion of it while all users in SSMA simultaneously utilize the channel fully to achieve the multiple access in addition to obtaining the above mentioned advantages [1].

The technique of SSM(A) can be explained as follows. Each user is assigned a spectrum spreading sequence which is near orthogonal to that of any other user. Such spectrally spread signals are added and transmitted over a channel (in SSM). At the receiver this composite signal is correlated with each of the SS sequences thus recovering individual user signals. The actual signal is recovered while all other

interfering signals are spread out so as to cause minimum
interference. The method is explained in detail in Chapter 3.
The bandwidth of the spreading signal is very large when
compared with the bandwidth of the information bearing signal
it spreads. The higher the ratio of the two bandwidths the
larger the advantage we gain by SS modulation. However, this
is not the case with the Additive White Gaussian Noise (AWGN)
environment, where SS modulation does not offer any advantage
over other schemes. Later we will have occassion to show
this.

The high bandwidth requirement of the SS modulation (or
SSMA) if used in a data network can be met by optical fibers.
In addition to this, many other advantages of the optical
fibers [2] led people to consider it as a medium for different
data networks [3],[4]. Both of them put together, SSMA in
optical fiber communications seems to be a good alternative
to the existing schemes. One such attempt is given in [3].
However, such a conclusion can only be made after analysing
the performance of SSMA in fiber optic communications. Unlike
the traditional communication systems, where the AWGN is the
fundamental limitation on ideal communication optical commu-
nication involves an additional fundamental source of noise,
namely the shot noise. It is inherent to the photodetection
process, at the receiver, by which the optical power is

converted to electric current. So a complete analysis is required to see the effect of such shot noise and the limitation it introduces into the system performance. This has not been considered in [3]. An attempt has been made here in this thesis to study this and arrive at the system performance of SSMA in fiber optic communication.

1.2 OUTLINE OF THE THESIS:

This thesis consists of five chapters. In Chapter 2 we scan through the problem of communication over a fiber optic channel and the two approaches taken by people to solve the problem of detection at the receiver.

In Chapter 3, the SS modulation and its capabilities are discussed. The multiple access situation and the performance limitation it introduces are also analytically presented. We also discuss briefly the different methods of SSMA.

In Chapter 4, we propose the receiver and evaluate the performance of the receiver. Both the cases of unlimited bandwidth and limited bandwidth are considered. Inverse filtering is proposed as a possible solution to the problem created by the bandwidth limitation at the receiver. The system for unlimited bandwidth case is simulated on a digital computer.

In Chapter 5, we present the results of the performance predicted in Chapter 4, along with the simulation results. The chapter concludes with a critical evaluation of the proposed system and the limitations of it and with suggestions for further work.

CHAPTER 2

DIGITAL FIBER OPTIC COMMUNICATION RECEIVERS

This chapter begins with a description of a general model of the digital fiber optic communication system. The model suggests the different signal processing schemes that can be implemented. We then discuss briefly the work done by others in this field previously.

2.1 THE FIBER OPTIC COMMUNICATION SYSTEM MODEL:

A general digital fiber optic communication system is as shown in Fig. 2.1. The information source puts out random binary data which are transmitted using a suitable pulse format. The typical pulse formats are PAM and PPM. They are as shown in Fig. 2.2. Other pulse formats can also be used. These pulses modulated by the data bits are fed to a LED or Laser which illuminates the fiber accordingly. If the intensity of the light incident is directly proportional to the signal pulse, it is called Intensity Modulation. This intensity modulated optical signal, can possibly be attenuated and distorted while travelling on the fiber, before reaching the receiver end.

At the receiver this optical signal can be processed in two ways. One is to take the electromagnetic considerations and process the light accordingly [6]. Such a method calls
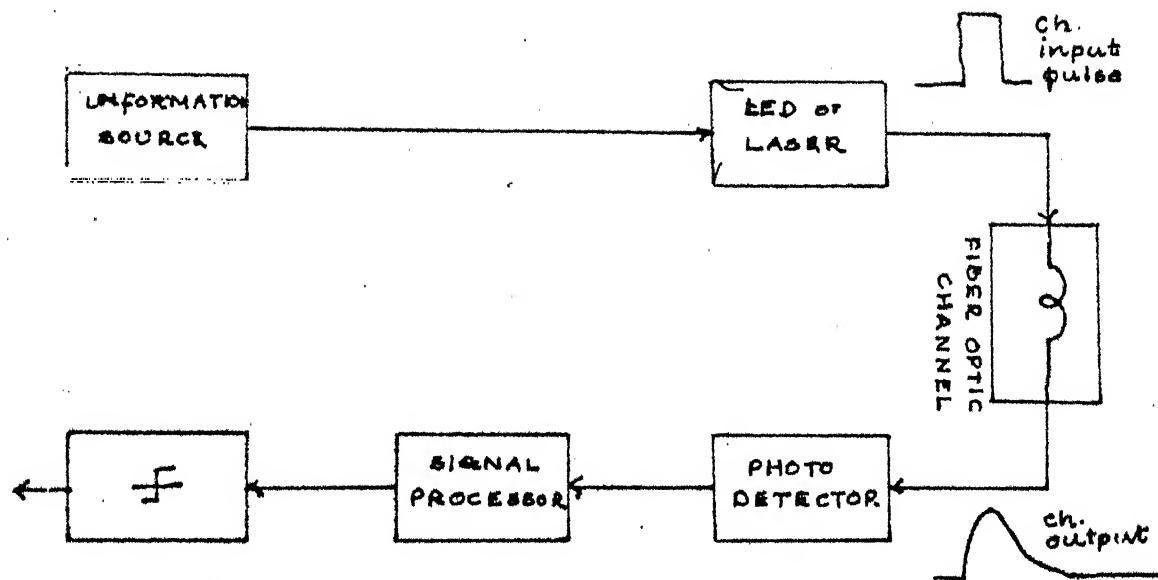
FIG. 2.1 GENERAL DIGITAL FIBER OPTIC COMMUNICATION MODEL

P.A.M.

P. P. M.
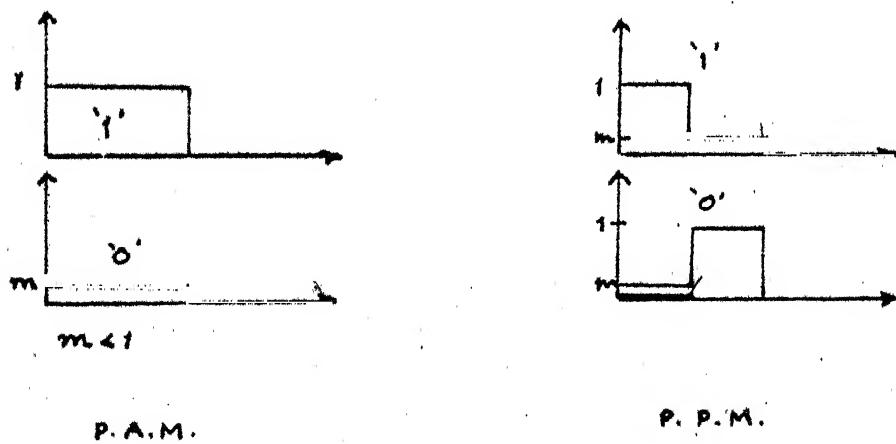
FIG 2.2 PULSE FORMATS

for coherently detecting the light. But these methods are complex and highly sensitive to allignment errors etc. The other method is to photo-detect the optical signal, i.e. converting the optical power into electric signal, prior to any signal processing. Such a scheme is known as 'Direct detection' method. A photo-detector, either a PIN diode or an Avalanche photo diode (APD) is normally used for this purpose. The former simply converts the optical signal into electric current without any amplification resulting in a low signal to noise ratio (SNR). The latter provides signal amplification resulting in a high SNR. In both cases they detect the signal as a noise process whose average value is related to the signal. This noise is known as shot noise and is of fundamental importance to the fiber optic communication problem. What distinguishes it from the regular thermal noise is its dependence on the signal. The average value of this process will be linearly related to the signal transmitted provided we assume that optical pulses add linearly. Such a case has been considered by Personick [5] and he shows the assumption to be true for multimode fibers. The photodetector has associated biasing circuitry and subsequent amplification of the signal also takes place. This front-end circuitry in addition to, possibly, distorting the detected signal, adds the thermal noise. At the circuit level the various noise sources can be as shown in Fig. 2.3.
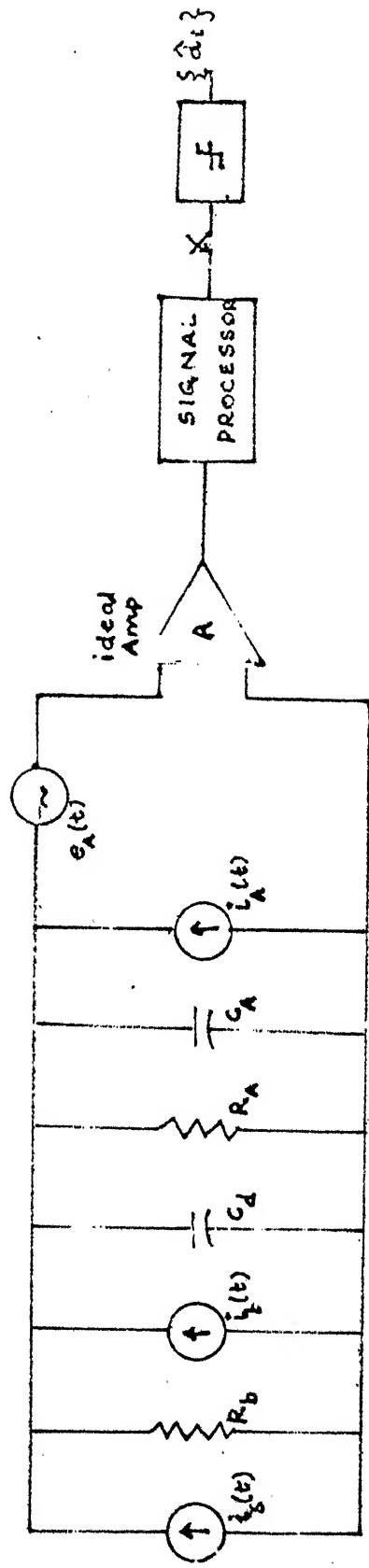
FIG. 2.3: RECEIVER MODEL WITH NOISE SOURCES SHOWN.

9

The thermal noise source associated with R_b is modelled as a shunt current source $i_b(t)$. The amplifier noise source, referred to the input are $i_A(t)$ and $e_A(t)$. They are followed by the noiseless ideal amplifier with gain A. The current source $i_s(t)$ 'the signal source' accounts for the shot noise current. It is actually a sequence of randomly located impulses whose emission times are governed by the intensity of the incident light, $\lambda(t)$. Specifically,

$$i_s(t) = \sum_{i=1}^{k(o,t)} e\, g_i \; (t-t_i) \qquad (2.1)$$

Where 'e' is the electron charge and g_i are the random gains provided by the APD (i.e. corresponding to each primary electron a bunch of g_i secondary electrons is released). The density function of g_i is usually complicated [15], but its moments can be calculated knowing the ionization constant of the photodetecting device. In case of a PIN diode $g_i \equiv 1$. t_i's are the random instants of time when an electron-hole pair is generated due to the absorption of a photon. $k(0,t)$ is known as the count variable and is equal to the number of electrons emitted during the interval $(0,t)$. Clearly $k(0,t)$ is a random variable. It has Poisson statistics with density [6]

$$p(k=n) = \frac{\lambda^n}{n!} \; e^{-\lambda} \qquad (2.2)$$

where $\lambda = \int_o^t \lambda(t)dt \qquad (2.3)$

which means that the probability of emission of n electrons
in the interval (o,t) is given by the above expression.

We know that intensity $\lambda(t)$ of the optical field depends
on the time varying optical power as

$$\lambda(t) = \frac{\eta}{h\gamma} p(t) + \lambda_o \qquad (2.4)$$

where η : photon counter efficiency

$\quad h\gamma$: energy of the photon

$\quad \lambda_o$: dark current intensity

and $p(t)$: is given by

$$p(t) = \sum_{i=-\infty}^{\infty} d_i h_p(t-iT) \qquad (2.5)$$

where d_i are data bits $\{0,1\}$ and $h_p(t)$ is the optical channel
output pulse as shown in Fig. 2.1.
T - data bit duration.

If $v_o(t)$ is the output of the amplifier of gain A, then

$$v_o(t) = A \sum_{i=1}^{k(o,t)} e\, g_i\, h_{fe}(t-t_i) + A(i_b(t) +$$

$$i_A(t))* h_{fe}(t) + A\, e_A(t) \qquad (2.6)$$

where $h_{fe}(t)$ is the impulse response of the front end RC
circuit, i.e. we have a composite signal which is the sum of
a shot noise term, whose average value is the signal desired

(we will show this latter) and three independent Gaussian noise terms. Now the problem is how should $v_o(t)$ be further processed so that the desired signal can be detected with reasonably good fidelity. Infact, certain amount of noise suppression can be done by properly choosing the front end circuitry itself. We will see the consequences of such a step later. Before that we go through the work previously done to solve the above problem.

In the literature basically two approaches are taken to process $v_o(t)$. One is to have $v_o(t)$ optimally processed. For this the likelihood function is evaluated and the resulting structure implemented. Such receivers are obtained by Bar-David [7], Gagliardi and Karp [6], and Foschini et.al. [8]. Bar-David has considered the problem with no ISI and AWGN free situation. Gagliardi and Karp considered the problem with no ISI and additive Poisson Noise. The structure arrived at by the former is a cascade of electron emission times estimator and a weighted photon counter. The Maximum A Posteriori (MAP) receiver derived by Gagliardi and Karp finds a pair of weighted sums of the observed count components and compares the sums to get the larger.

Foschini et.al. considered pulse dispersion also and they obtained a receiver which is a cascade of two viterbi

algorithm (VA) receivers, one to estimate the electron emission times and the other to estimate the data sequence in the presence of ISI [9]. The impracticality of VA structure at high data rates led to the consideration of the possible use of Decision Feedback Equalizer (DFE) in its place. Such a suboptimal structure was obtained by Govind Sharma [10]. However this structure also requires high sampling rates at the receiver which again limits the data rates. It also requires a high signal to noise ratio. The ISI problem is also considered by Dogliotti et.al. [11] in which either a transversal filter or a Kalman filter is offered as the receiver structure. Shot noise was not considered in this. Messerschmitt [12] also arrived at the cascade of a forward filter and a DFE which minimized the mean square error. In the last two works performance evaluation in terms of probability of error was not done.

The other approach is to suboptimally process the $v_o(t)$ by assuming a receiver structure which does not consider the discrete nature of the shot noise to find the optimal structure like the first approach. However, the complexity of the optimal receivers led to this approach. Thus the work of Personick [13] proceeds this way where he obtains a linear solution to this problem. He takes $v_o(t)$ and passes

it through an equalizer which eliminates the ISI comple-
tely (zero forcing) at the sampling instants by selecting
the output pulse shape to be a raised cosine. Unlike the
above methods where the exact method (of finding the
density of the decision statistic) is used to find the
performance, here only the Gaussian approximation (or the
signal to noise ratio approx.) is used to find the perfor-
mance, i.e. the probability of error. He argues that for
practical systems of interest results obtained from such
calculation differ by about 2 db from the ones found by the
exact method.

In this thesis we attempt to solve our problem on the
lines of second approach. The explicit statement of the
problem is: How do we process $v_o(t)$ and obtain the performance
of such a processor when $v_o(t)$ is owing to the sum of K
asynchronous SS modulated signals. The system can be shown
as in Fig. 2.4. The suboptimal solution is sought for the
reasons that in the case of AWGN its performance is reasonably
good and the complexity of the receiver is also small. A
fiber optic SS modulation case has been considered earlier in
[14] with no multiple access and no ISI. The receiver given
there does not suit for our case for reasons explained in the
next chapter. Before going on to propose the actual receiver
structure we discuss in the next chapter the various capabi-
lities of SS modulation and SSMA techniques.
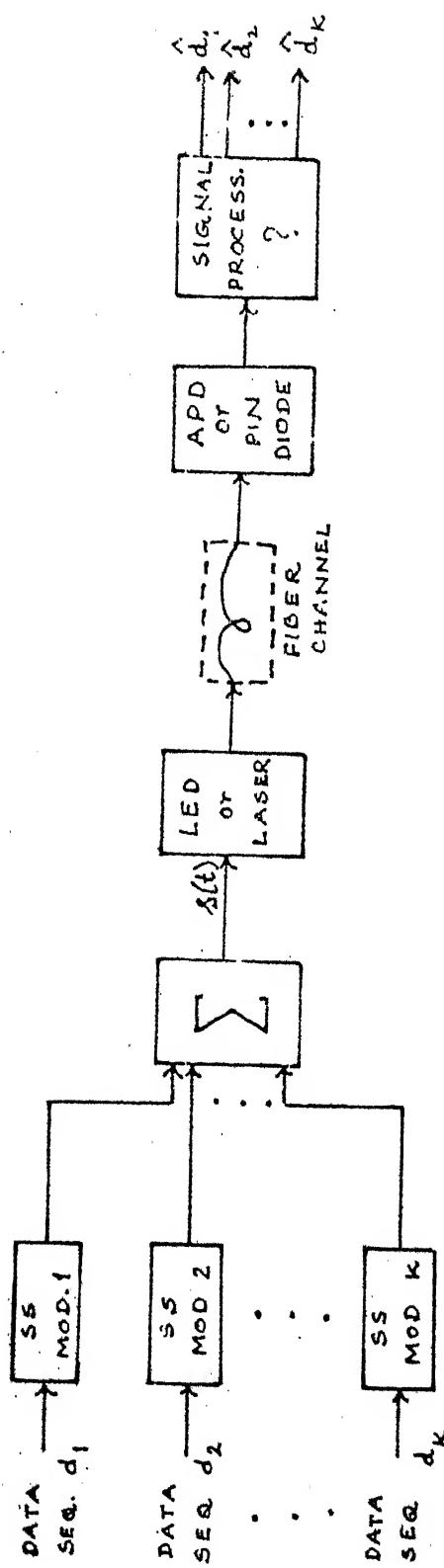
FIG 2.4 FIBER OPTIC SSMA SYSTEM

CHAPTER 3

SPREAD SPECTRUM MULTIPLE ACCESS COMMUNICATION SYSTEMS

In this chapter we first present the various
capabilities of the SS modulation. After that we give the
reasons for choosing this Multiple Access method instead of
TDMA or FDMA. Lastly we give the Multiple access system model
(without any reference to fiber optic communication) and presen
the analysis for quantifying the multiple access interference.

3.1 SPREAD SPECTRUM COMUNICATION USING A RANDOM SIGNAL MODEL :

The concept of Spread Spectrum (SS) communication and
its Multiple Access method can be easily understood by assuming
that the signals used for spreading of the incoming data
sequences are random processes, which are not suited for system
implementations. For this reason, in what follows, we will
not give a too mathematical treatment. A more precise analysis
will be presented after this for a specific system model which
is implementable.

Let $c(t)$ be a zero mean stationary Gaussian random
process which has autocorrelation function $R_c(\tau)$ given by

$$R_c(\tau) = (T_c)^{-1}(T_c - |\tau|), \quad |\tau| \leqslant T_c$$

$$= 0 \qquad\qquad |\tau| > T_c \qquad (3.1)$$

The actual shape of $R_c(\tau)$ is not important as far as it is approximately zero out side (o, T_c). Its spectral density $S_c(f)$ is given by

$$S_c(f) = T_c [sinc(fT_c)]^2 \qquad (3.2)$$

Let $s(t)$ be a binary data signal, of duration T and constant amplitude $\pm A$ ($A>o$). We assume $T>>T_c$. Consequently the bandwidth of $c(t)$ is large compared to that of $s(t)$. Assume a noiseless baseband channel over which we send the SS modulated signal, $s(t) c(t)$, and use a correlator in the receiver to recover $s(t)$. The decision statistic is

$$Z = \int_0^T [s(t)c(t)]c(t)dt = \int_0^T s(t)c^2(t)dt = \pm A \int_0^T c^2(t) \, dt$$

$$s(t) \, \varepsilon \, \{A, -A\}$$

Ergodicity implies that with high probability

$$T^{-1} \int_0^T c^2(t)dt = E[c^2(t)] = R_c(o) = 1$$

$$Z = \pm AT$$

Thus $s(t)$ is recovered exactly in the absence of channel noise. However it is to be noticed that, for this recovery, the knowledge of $c(t)$ at the receiver is necessary which makes this conceptual model nonimplementable. Usually $c(t)$ is

approximated by a pseudo noise (PN) waveform derived from a PN-sequence. We now consider the effect of interfering signals on this SS communication system which we claimed in the first chapter to be reduced due to SS modulation.

1. Anti-Interference capability:

Let the received signal be

$$f(t) = s(t)c(t) + A'$$

where A' – d.c. signal

Now,

$$Z = \int_0^T s(t)\ c(t)dt + A' \int_0^T c(t)dt$$

$$= \pm AT + A'T \left\{ T^{-1} \int_0^T c(t)dt \right\}$$

The interference is negligible if $\frac{A'}{A}\ \frac{1}{T} \int_0^T c(t)dt \approx 0$ which is true if $A' \approx A$ since $c(t)$ has zero mean and T is large compared to T_c. Thus it can reject the d.c. interfering signal. By using similar argument one can show that it has a.c. interference rejection capability by making use of this fact that

$$\frac{1}{T} \int_0^T c(t)\ \cos \omega_0 t\ dt \approx 0$$

where ω_0 is the frequency of the a.c. tone.

2. Anti-Multipath Capability:

In a simplified base band model of a single multipath

channel the received signal might be

$$r(t) = s(t)c(t) - \beta s(t-\tau)c(t-\tau), \quad 0 \leq \beta \leq 1$$

If $s(t) = A$ for (o,T) and $\tau > T_c$

$$Z = \int_o^T r(t)c(t)dt = AT - \beta A \int_o^T c(t) \, c(t-\ ) \, dt$$

$$\approx 1 - \beta R_c(\tau)AT \quad AT$$

Thus if the multipath delays are greater than T_c they do not affect the performance of the system.

3. Multiple Access Capability:

Let there be K transmitted signals, each with a different process $c_k(t)$, $1 \leq k \leq K$. The processes are mutually independent. The received signal is

$$r(t) = \sum_{k=1}^K s_k(t) \, c_k(t)$$

The output of the ith correlator is

$$Z_i = \int_o^T r(t) \, c_i(t)dt \qquad (3.3)$$

$$= \int_o^T s_i(t)c_i(t)dt + \sum_{\substack{k=1 \\ \neq i}}^K \int_o^T s_k(t)c_k(t)c_i(t)dt$$

$$= \pm AT + \sum_{\substack{i=1 \\ \neq k}}^K \pm A \int_o c_k(t)c_i(t)dt$$

Since

$c_k(t)$, $c_i(t)$ are independent zero mean processes

$$T^{-1} \int_0^T c_k(t) c_i(t) dt \approx 0$$

$Z_i = \pm$ AT. This demonstrates the multiple Access capability of SS modulation.

In all the above cases, the key feature is that the c(t) has low correlation with the interfering signals. Thus it produces only a negligible change in the output of the correlation receiver. The integrator tends to 'smooth' the interfering signals, but it produces a large peak in response to the desired signal. Such an explanation can also be given in terms of frequency domain.

In addition to the above it can be shown that SS modulation can also combat narrowband, partial band interferences [1].

3.2 SYSTEMS OF SS COMMUNICATIONS:

There are mainly three methods and some combinations of them to implement the normal SS communication system they are:

1. Pseudo Noise Sequence modulation

2. Frequency Hopping modulation

3. Time Hopping modulation

In the first method the spreading of the spectrum is achieved

by multiplying the data signal by a (usually) binary PN – sequence. This is also known as direct sequence SS modulation. This system is easier to implement. The second method uses a pseudo random assignment of the carrier frequency of the base band data modulated signal such that the signal in frequency domain sweeps the frequency band by hopping in a pseudo random way. These are relatively difficult to implement due to the difficulty in implementing the frequency synthesizers with such a wide range. The third method, namely the Time hopping, transmits the signal only at selected intervals (varying) of time chosen in a pseudo random way. It has an advantage that the average power requirement is less. Normally a combinations of any two of the above seems most useful. Many such systems are given in [26], [27], [28]. In the next section we consider the first method, i.e. PN – sequence modulation with reference to Multiple Access situation.

3.3 DIRECT SEQUENCE SPREAD SPECTRUM MULTIPLE ACCESS COMMUNICATION:

Before going on to describe the SSMA, we give a heuristic argument for choosing SSMA as opposed to TDMA or FDMA. In an ideal condition all the three offer equal number of users for a given system bandwidth. However, when other aspects such as fading due to multipath, interference from

other communication systems, intentional jamming etc. affect the performance, the use of SSMA over the others proves useful. The other important advantage of SSMA over TDMA is that it can be operated in an asynchronous manner (i.e. users are asynchronous), a fact which makes us prefer SSMA to TDMA because of the costlier synchronizing equipment needed in case of the latter in a Multiple Access environment. Especially in data networks this asynchronous mode of operation can also be exploited in terms of reducing the complexity of network protocols. In fiber optic communication, the effects of nonlinearities of the transmitting and receiving devices reduce the performance of FDMA where as SSMA has the capability to reduce their effect [3]. For these reasons the SSMA seems to be a viable alternative to the other two.

However it should be noted that the advantages of SS communication are not present in some situations. For example in a purely AWGN environment (no other source of interference is present) the use of SS modulation offers no advantage. To see this, let the received signal be

$$r(t) = d(t)a(t) + \omega(t); \quad d(t) - \text{message signal}, \pm 1,$$

$$a(t) - \text{PN sequence}, \omega(t) - \text{AWGN zeromean variance} = \frac{N_0}{2}$$
$$\pm 1$$

As usual we use the correlator to recover the data

$$Z = \int_0^T r(t)a(t)dt = d_0 T + \omega_i \tag{3.4}$$

$$E[Z/d_0 = +1] = T \; ;$$

$$Var[Z^2] = \int_0^T \int_0^T a(t_1)a(t_2)E[\omega(t_2)\omega(t_1)]\partial t_1 dt_2$$

$$= \frac{N_0}{2} \int_0^T \int_0^T a(t_1)a(t_2) \delta(t_1-t_2)\alpha t_1 \; \alpha t_2 = \frac{N_0}{2} T$$

$$P_e = erfc^*(d) \text{ where } d^2 = \frac{E^2(Z)}{Var(Z)} = \frac{2}{N_0} T$$

Thus it has nothing to offer as an advantage over BPSK modulation scheme in this situation.

The effect of shot noise on the SS communication will be seen in the next chapter. We now give the multiple Access situation with its interference effects with no other additive noise sources.

Binary Baseband SSMA Communication:

In binary direct sequence form of SS modulation, a baseband signal of the form

$$x(t) = \sum_{j=-\infty}^{\infty} x_j P_{T_c}(t- jT_c) \tag{3.5}$$

is employed as the spectral spreading signal. In the above, sequence (x_j) is a periodic sequence of elements $\{+1, -1\}$

and $P_{T_c}(t)$ is a time limited signal [limited to (o, T_c)] for which

$$T_c^{-1} \int_0^{T_c} P_{T_c}^2(t)dt = 1 \qquad (3.6)$$

The normal choice for fibre optic communication would be

$$P_{T_c}(t) = 1 \qquad 0 \leq t \leq T_c$$
$$= 0 \qquad \text{otherwise}$$

$P_{T_c}(t)$ is commonly referred to as chip waveform. The sequence $x = (x_j)$, called the signature sequence when employed for a particular user signal, is periodic with period N. i.e. $x_j = x_{j+N}$ for each j.

The binary data signal waveform d(t) is given by

$$d(t) = \sum_{\ell=-\infty}^{\infty} d_\ell P_T(t - \ell T) \qquad (3.7)$$

where $P_T(t)$ is non-zero over $[o, T]$. d_ℓ is the binary random sequence $\{+1, -1\}$ corr. to the user signal. When x(t) is used as a signature sequence for d(t), N is normally chosen to be equal to T/T_c i.e. T is an integer multiple of T_c. So, for each data bit, a period of the sequence is modulated by each data bit d . Therefore the bandwidth of x(t) is of the order of N times that of d(t). With this, we now give the SSMA model.

As shown in Fig. 3.1, the SSMA has K asynchronous
users $d_i(t)$ each with a random delay τ_i. Each of these
are modulated with synchronous (to the particular d(t))
PN-sequences $a_i(t)$ and are linearly added to form a composite
signal s(t)

Fig. 3.1: Baseband SSMA communication system

$$s(t) = A \sum_{i=1}^{K} d_i(t- \tau_i)a_i(t- \tau_i) \qquad (3.7)$$

$$=. \sum_{i} s_i(t)$$

The PN-sequences $a_i(t)$ are chosen so as to approximate the
c(t) of section 3.1, so that their cross correlation and
out of phase autocorrelations values will be small. At the
receiver s(t) is $\angle$ corrupted by noise n(t) (in traditional
systems n(t) is AWGN plus any other interferences present)
which in our case will be sum of thermal and shot noises.

As shown in Fig. 3.1, the SSMA has K asynchronous users $d_i(t)$ each with a random delay τ_i. Each of these are modulated with synchronous (to the particular $d(t)$) PN-sequences $a_i(t)$ and are linearly added to form a composite signal $s(t)$

Fig. 3.1: Baseband SSMA communication system

$$s(t) = A \sum_{i=1}^{K} d_i(t - \tau_i) a_i(t - \tau_i) \qquad (3.7)$$

$$=. \sum_{i} s_i(t)$$

The PN-sequences $a_i(t)$ are chosen so as to approximate the $c(t)$ of section 3.1, so that their cross correlation and out of phase autocorrelations values will be small. At the receiver $s(t)$ is corrupted by noise $n(t)$ (in traditional systems $n(t)$ is AWGN plus any other interferences present) which in our case will be sum of thermal and shot noises.

For the moment, we neglect their effect and consider only the multiple access interference. It is to be noted that all the users are assumed to have equal amplitude A. In such a case the detection of chips of each sequence and thereby the the data bits is not possible as the signal to interference ratio is far less than unity $(\frac{1}{K-1})$. For this reason the receiver proposed for the SS modulated signal in fiber optic communication in [14] is not applicable here. The equal power situation can be generalised to different amplitude levels A_i (more appropriate for Multiple Access situation where the 'near-far' problem comes into picture) which modifies s(t) as s(t) = $\sum_{i=1}^{K} A_i d_i(t-\tau_i)a_i(t-\tau)$. It is also assumed that $\tau_i's$ are uniformly distributed over (o,T). For analysis purpose, we consider the receiver to be synchronised to user one signal that τ_1 can be assumed to be zero as shown.

$$r(t) = Ad_1(t)a_1(t) + A\sum_{i=2}^{K}d_i(t-\tau_i)a_i(t-\tau_i)$$

We assume the receiver to be a correlation (or matched filter) receiver. The output of this receiver is

$$l = \int_o^T r(t)a_1(t)dt = A\int_o^T d_1(t)a_1^2(t)dt$$

$$+ A\sum_{i=2}^{K}\int_o^T d_i(t-\tau_i)a_i(t-\tau_i)a_1(t)dt$$

$$= Ad_{1,o}T + A\sum_{i=2}^{K}(d_{i,-1}\int_o^{\tau_i}a_i(t-\tau_i)a_1(t)dt + d_{i,o}$$

$$\int_{\tau_i}^T a_i(t-\tau_i)a_1(t)dt) \tag{3.8}$$

which is clear from the figure shown in Fig. 3.2. The integrals in eq. (3.8) are given by

$$R_{i,1}(\tau) = \int_0^\tau a_i(t - \tau_i)a_1(t)dt$$

$$R_{i,1}(\tau) = \int_\tau^T a_i(t - \tau_i)a_1(t)dt$$
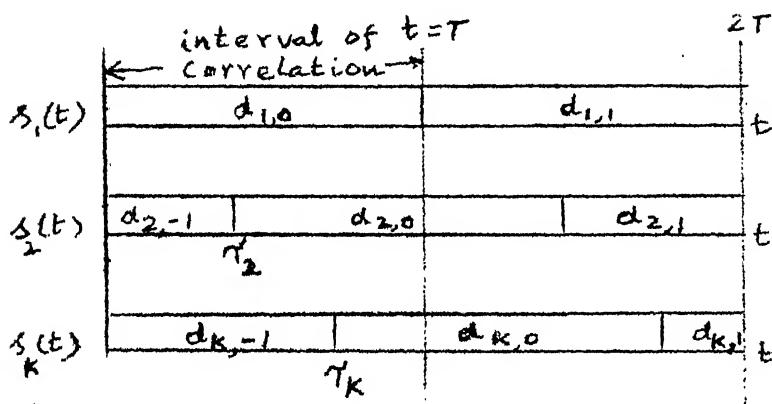
Figure 3.2: AAsynchronous data sequences.

which are known as continuous time partial cross correlation functions. These were introduced in [16] and used in the analysis of binary direct sequence SSMA communications [16],[17] Their effect on the receiver output is via the quantity.

$$I_{k,1}(d_i, \tau) \doteq T^{-1}[d_{i,-1}R_{i,1}(\tau) + d_{i,o}R_{i,1}(\tau)]$$

$$(3.9)$$

which is referred to as the (normalized) multiple access interfe ence at the output of the first receiver due to the ith signal. The vector d_i is the vector $(d_{i,-1}, d_{i,o})$ of two consecutive

data bits of the ith data source. Therefore ℓ_1 can be written as

$$\ell_1 = AT \left[d_{1,o} + \sum_{i=2}^{K} I_{i,1}(d_i, \tau_i) \right] \qquad (3.10)$$

It is clear for K=1 (i.e. no Multiple Access), the summation term is not present. In that case, in the presence of AWGN, ℓ_1 is the sufficient statistic [18] and we decide the first user data bits by comparing ℓ_1 with zero for optimum detection. For K>1, it is not the sufficient statistic and a more complex receiver can provide a statistic which gives near optimal decision. However since correlator receivers are relatively single to implement, the vast majority of direct sequence SSMA systems employ correlation receivers, even though they are suboptimal. This is because of the relatively small performance improvement that can be obtained with a more complex receiver.

The usual performance criterion, the probability of error can be evaluated using two criteria. One is to find the maximum value of the multiple access interference (worst case value) and find the P_e in the presence of AWGN. Such a method is taken in [16] and expressions for worst case value of multiple access interference (MAI) obtained. The other is to consider the mean square value of MAI which leads to signal to noise ratio as a measure of performance. We now

proceed to obtain its value. The reasons for taking this step will be clear later. In general the first one is not preferred because the worst case MAI occurs very infrequently.

Let,

$$\underline{d} = (d_{2,-1}, d_{2,o}, d_{3,-1}, d_{3,o} \cdots d_{k,-1}, d_{k,o});$$

$$\underline{\tau} = (\tau_2, \tau_3, \quad \ldots \tau_k)$$

we can assume $\underline{d}$, $\underline{\tau}$ to be independent as they arise from independent physical phynomena. We also assume $d_{i,j}$ and $d_{m,n}$ to be independent for all $i \neq m$ and $j \neq n$, and so are the τ_i, τ_j for $i \neq j$. From these independence assumptions, we see

$E[I_{i,1}(d_i, \tau_i)] = 0$. Since $P(d_{i,-1} = +1) = P(d_{i,o}) = 1/2$,

the variance of $I_{i,1}(d_i, \tau_i)$ is given by

$$\sigma_{i,1}^2 = \text{Var}\ [I_{i,1}(d_i, \tau_i)] = T^{-2} \int_o^T T^{-1}\ [\widehat{R}_{i,1}^2(\tau) + \widehat{R}_{i,1}^2(\tau)]d\tau$$

$$(3.11)$$

Defining the quantities $\quad m_{i,1} = \int_o^T R_{i,1}^2(\tau)d\tau \ ; \ \widehat{m}_{i,1} = \int_o^T \widehat{R}_{i,1}^2(\tau)d$

we have

$$\sigma_{i,1}^2 = T^{-3}(m_{i,1} + \widehat{m}_{i,1}) \tag{3.12}$$

The quantities $m_{i,1}$, $m_{i,1}$ are analysed and closed form expressions are obtained in [19]. Using those expressions, $\sigma_{i,1}^2$ can be written as

$$\sigma_{i,1}^2 = (3N^3)^{-1} \left[2 \mu_{i,1}(0) + \mu_{i,1}(1) \right] \tag{3.13}$$

where the parameter $\mu_{i,j}(n)$ is given by

$$\mu_{i,j}(n) = \sum_{\ell=1-N}^{N-1} C_i(\ell) C_j(\ell + n) \tag{3.14}$$

where $C_i(\ell)$, $C_j(\ell)$ are the aperiodic autocorrelation functions [16] of the i and jth signature sequences respectively. They are given by

$$C_i(\ell) = \sum_{j=0}^{N-1-\ell} a_j^{(i)} a_{j+\ell}^{(i)}, \quad 0 \le \ell \le N-1$$

$$= \sum_{j=0}^{N-1+\ell} a_{j-\ell}^{(i)} a_j^{(i)}, \quad 1-N \le \ell < 0$$

$$= 0, \quad |\ell| \ge N$$

More generally,

$$C_{k,i}(\ell) = \sum_{j=0}^{N-1-\ell} a_j^{(k)} a_{j+\ell}^{(i)}, \quad 0 \le \ell \le N-1$$

$$= \sum_{j=0}^{N-1+\ell} a_{j-\ell}^{(k)} a_j^{(i)}, \quad 1-N \le \ell < 0$$

$$= 0, \quad |\ell| \ge N \tag{3.15}$$

and $C_i(\ell) = C_{i,i}(\ell)$

where $a_j^{(i)}$ is the jth chip element of the ith sequence. Note that $C_i(\ell) = C_i(-\ell)$, $\ell > 0$.

Thus from eqs. (3.13) to (3.15) it can be seen that $\sigma_{i,j}^2$ for all i and j $(i\neq j)$ can be found knowing only K Autocorrelation functions $C_i(\ell)$ of the PN sequences and K^2 cross correlation functions $C_{k,i}(\ell)$ are not required. With increasing sequence length N, computation of $\sigma_{i,1}^2$ takes more and more time. So some bounds are considered in [20] to minimize this time.

Once knowing the $\sigma_{i,1}^2$ and the (possible) AWGN variance $\sigma_{th}^2 T$ we can find the signal to noise ratio as

$$d^2 = \frac{A^2 T^2}{A^2 T^2 \sum_{i\neq 1} \sigma_{i,1}^2 + \sigma_{th}^2 T} = \frac{A^2}{A^2 \sum \sigma_{i,1}^2 + \sigma_{th}^2/T}$$

and the approximate probability of error (suggested by Pursley [16]) is $P_e \approx erfc^*(d)$. The accurate evaluation of P_e can be found in [21] and in that the author shows this signal to noise ratio approximation is very close to the accurate value when the number of users is large and the users are asynchronous, with high signal to noise ratio. We will examine the accuracy of this approximation in Chapter 5 by performing simulations of the system.

Before concluding this chapter, we mention briefly about the selection of the above PN-sequences. For a given N

of reasonable length the Max. length sequences are relatively small in number. For example for N=511 they are 24. For N = 1023 they are 30. So as an alternative to these, we consider other sequences with these periods. Two of them are Gold Sequences and Kasami Sequences [22]. For every N = 2^n-1, n ≠o mod 4 there exist 2^n+1 Gold sequences with period N. In Kasami Sequences there exist 2 classes, one is the smaller class and the other is the larger class. In the smaller class there are $2^{n/2}$ sequences with period N = 2^n-1. In the larger class there exist $2^{n/2}(2^n+1)$ sequences with period same as N. Earlier, these sequences were found for the following reason.. When synchronous users are present, the Multiple Access interference (not the quantity defined above) depends on the periodic cross correlation of the user PN-sequences [22]. The Gold and Kasami sequences were obtained in an effort to reach the lower bounds of their cross-correlations in such a situation. With M sequences such bounds are met for only a few selected pairs of sequences known as preferred pairs. Quantitatively this bound [22] is given by

$$\theta_{i,j}(\lambda) \geq 2^{(n+1)/2} + 1, \quad n \text{ odd}$$

$$\geq 2^{(n+2)/2} + 1, \quad n \text{ even}$$

For Gold sequence   the equality is satisfied provided
n is $\neq$ o mod 4.

    In the present asynchronous case, however, no such
sequences optimal with respect to **interference variance** $\sigma_{i,1}^2$
are known till now except for a class of M-L sequences of
length 31 to the best of this author's knowledge. So, for
the problem at our hand, we have chosen Gold sequences
considering their number. The selection and generation of
the Gold sequences are given in Appendix A.

CHAPTER 4
FIBER-OPTIC SSMA RECEIVER

In this chapter we propose the receiver for the problem stated earlier in Chapter 2 and analyse its performance for various cases. In the first section, the case of unlimited bandwidth will be analysed. The next one is to assume an equivalent band limited channel and see how the proposed receiver for the previous case be modified to get satisfactory performance. This will be discussed in the second section.

4.1 SSMA IN UNLIMITED BANDWIDTH CASE:

The system model is redrawn with the proposed receiver as shown, for this case in Figure 4.1. The users' data sequences are $d_1(t)$, $d_2(t)$... $d_k(t)$. For analysis purposes, only the detection of user 1 sequence, namely $d_1(t)$ will be considered as all the others will also go through same receiver operation. It is assumed that perfect synchronization exists between each pair of SS modulator and correlator corresponding to each user PN-sequence. The validity and consequences of such an assumption are discussed in Chapter 5. Since we are considering user 1, we make $\tau_1 = 0$ without loss of generality. Each of τ_i, $2 \leq i \leq K$ is uniformly distributed in (o, T), where T is the data bit duration. The user sequences are SS modulated by the respective SS carriers

FIG 4.12 FIBER OPTIC SSMA RECEIVER
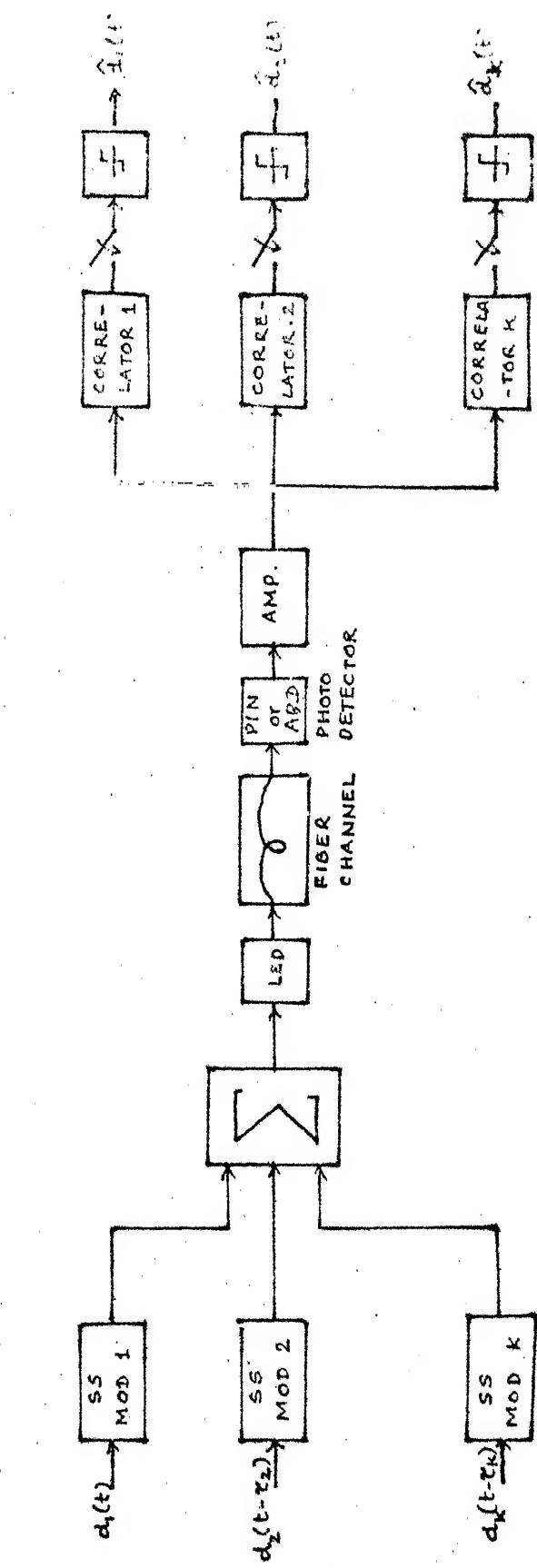
$a_1(t)$, $a_2(t)$...$a_k(t)$ and summed up. This composite signal is fed to an LED (or Laser) which drives the fiber with an intensity modulated optical signal. The optical power of that signal is linearly related to the input driving current of the LED over a wide range of input current.

In the fiber of unlimited bandwidth, the optical signal gets only attenuated while travelling, before arriving at the receiving end. At the receiver, prior to any signal processing, we let the optical signal be directly detected using the photodetector, either an APD or a PIN diode, as the case may be. With the former there is an amplification of the signal, though with an increased noise, in the process of detection whereas in the latter such an amplification is not present. Thus the signal to noise ratio (SNR) is larger in the former case than in the latter. The optimal amplification required can be derived. The detected signal is amplified and correlated to get signal statistic and is compared with threshold to decide the data bits. To see the operations, which the signal undergoes, we consider the equivalent models of the detector and amplifier and the correlator. They are as shown in Figure 4.2.

The photodiode is modelled as a current source $i_s(t)$ which accounts for the shot noise due to the emitted impulses of electrons at random time instants. C_d represents the
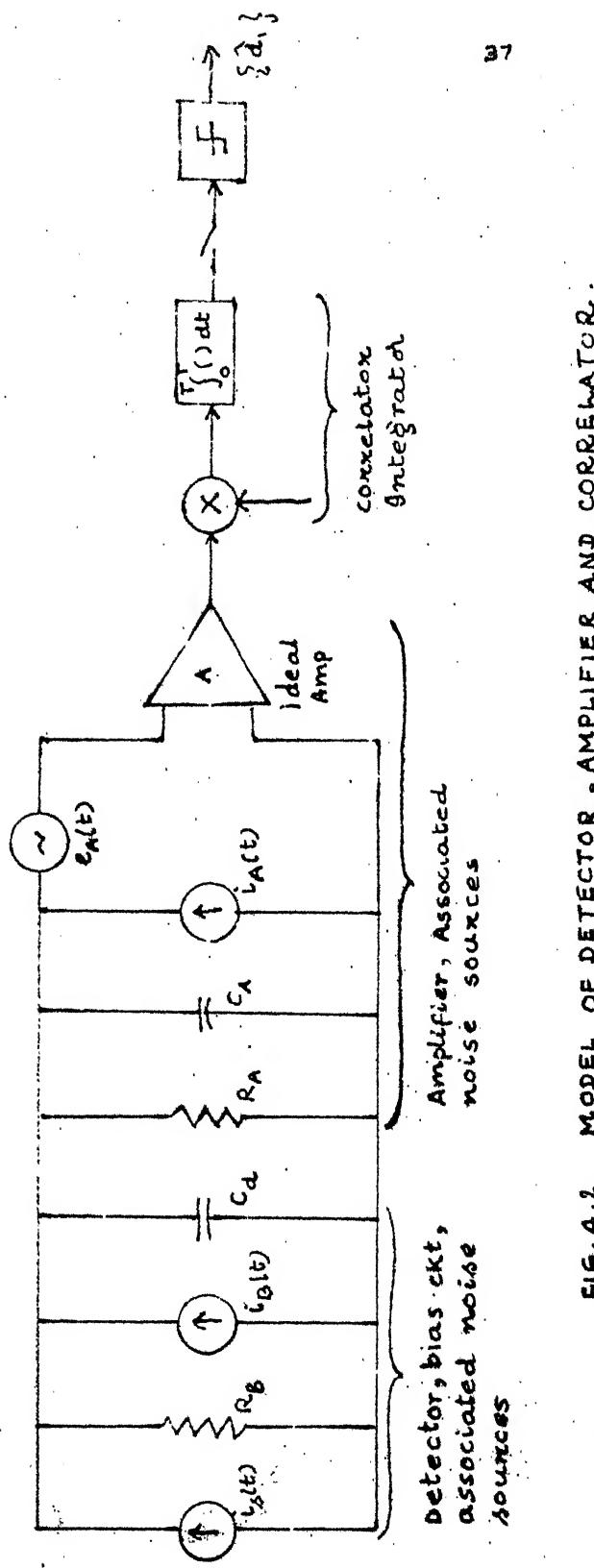
FIG. 4.2   MODEL OF DETECTOR, AMPLIFIER AND CORRELATOR.

diode junction capacitance. R_b is the bias resistance with its associated thermal noise current source $i_b(t)$ with power spectral density (p.s.d.) S_b Amp^2/Hz. R_A is the amplifier input resistance with the associated noise source $i_A(t)$ with p.s.d. S_A Amp^2/Hz. C_A is the Amplifier input capacitance $e_A(t)$ is the series noise source with p.s.d. S_E volt^2/Hz. Other models of amplifier can be taken, but the basic approach is the same.

The shot noise current source $i_s(t)$ is given by

$$i_s(t) = \sum_{i=1}^{k(o,t)} e\, g_i\, \delta(t-t_i) \qquad (4.1)$$

where g_i — Random gain of the APD

t_i — random time instants at which electrons are emitted

$k(o,t)$ — count variable representing the total number of electrons emitted in $)(o,t)$

$$v_s(t) = i_s(t) * h_{fe}(t)$$

$$= \sum_{i=1}^{k(o,t)} e\, g_i\, h_{fe}(t-t_i) \qquad (4.2)$$

where $h_f(t)$ = impulse response of the biasing plus amplifier circuitries with time constant RC where

$$R = R_A || R_B;\ C = C_A + C_d,$$

i.e. $h_{fc}(t) = \frac{1}{C}\, e^{-t/RC}$

The means and autocorrelations of $i_s(t)$ and $v_s(t)$ are given by [6]

$$E[i_s(t)] = \frac{\eta}{h\gamma} e \langle g \rangle \lambda(t) + \lambda_o e \langle g \rangle \qquad (4.3)$$

where,

η — quantum efficiency

h — planck's constant

γ — frequency of the light used

e — electron charge

$\langle g \rangle$ — Average value of the APD gain

λ_o — Dark current intensity

$\lambda(t)$ — is the time varying intensity of the incident optical field which depends on the composite SS signal. It is given by

$$\lambda(t) = \frac{\eta}{h\gamma} p(t) = \frac{\eta}{h\gamma} \cdot \frac{b_E}{T} (K + \sum_{i=1}^{K} d_i(t-\tau_i)a_i(t-\tau_i))$$

$$(4.4)$$

where $p(t)$ is the received optical power, b_E is the bit energy parameter which is related to the signal power at the transmitter as given below. T is the data bit duration.

At the transmitter we have the composite SS signal as

$$s_{in}(t) = \sum_{i=1}^{K} d_i(t-\tau_i)a_i(t-\tau_i)$$

It is assumed that $d_i \, \varepsilon \{+1,-1\}$, $a_i \, \varepsilon \{+1,-1\}$ and

$$\int_0^T a_i^2(t)dt = T.$$

To this we add a d.c. signal of K units to get $s(t) = K + s_{in}(t)$ which varies in $[0,2K]$ unlike $s_{in}(t)$ which varies in $[-K,K]$. We use this signal to, drive the LED/Laser. Since the input signal to an LED is in terms of its drive current , we assume

$$I(t) = I[K + \sum_{i=1}^{K} d_i(t - \tau_i)a_i(t - \tau_i)],$$

I is the current in Amps. The emitted optical power is related to this current by

$$p(t) = Q\, I(t)$$ where Q is the responsivity (watts/Amps) of the LED/Laser

$$= QI\, [K + \sum_{i=1}^{K} d_i(t - \tau_i)\, a_i(t - \tau_i)]$$

So letting $b_E = QIT$ (we multiplied by T since b_E is energy parameter), we have

$$p(t) = \frac{b_E}{T} (K + \sum_i d_i(t - \tau_i)\, a_i(t - \tau_i))$$

T is retained in the denominator only to give an idea of the power required, since $\frac{b_E}{T}$ has units of power. We now continue to find the expression for the mean of the shot noise process $v_s(t)$.

$$E[v_s(t)] = e\langle g\rangle \lambda(t) * h_{fe}(t) \tag{4.5}$$

neglecting the dark current intensity.

$$R_i(t_1, t_2) = E[i_s(t_1)i_s(t_2)] = e\, E[g_i^2]\, \lambda(t_1)\delta(t_1 - t_2)$$

$$+ E[i_s(t_1)]\, E[i_s(t_2)] \tag{4.6}$$

Let $E[g_i^2] = \langle g^2\rangle$

$E[g] = \langle g\rangle$

$$R_v(t_1, t_2) = E[v_s(t_1)v_s(t_2)] = e\langle g^2\rangle \int \lambda(\tau) \cdot$$

$$h_{fe}(t_1 - \tau)\, h_{fe}(t_2 - \tau)\, d\tau + E[v_s(t_1)] \cdot$$

$$E[v_s(t_2)] \tag{4.7}$$

Thus it is seen due to the non-stationarity of the process, the mean and autocorrelation functions of $i_s(t)$ and $v_s(t)$ are time dependent. We need these expressions in finding the SNR at the output of the correlator. In what follows, we consider that the fiber is dispersionless in time (i.e. causes No ISI) and analyse the system for two cases. The first is that the front end circuitry also does not spread the pulse. R and C are adjusted so as to make this condition prevail. In the second case, we consider the pulse spreading due to the front end. The reason for

introducing such deliberate dispersion will be clear when we
analyse the first case. We now go ahead to do this.

Let $v_o(t)$ be the output of the amplifier with gain A.
It is given by

$$v_o(t) = A\ v_s(t) + Av_g(t) + Ae_A(t) \tag{4.8}$$

where $v_g(t) = [i_b(t) + i_A(t)\ ] * h_{fe}(t)$ $\qquad$ (4.9)

is the Gaussian noise contribution. It may not be white
depending on $h_{fe}(t)$
or

$$v_o(t) \ = A\ i_s(t)*h_{fe}(t) + A(i_b(t) + i_A(t))*h_{fe}(t) + Ae_A(t)$$

we now assume $h_{fe}(t)$ is impulsive and is given by $h_{fe}(t) = R\delta(t)$.
Therefore

$$v_o(t) = AR\ i_s(t) + AR(i_b(t) + i_A(t) + A\ e_A(t)$$

We can write $i_s(t)$ as sum of an average component $\langle i_s(t)\rangle$
and a noise component $i_s(t)$ (to minimize notation we retain
$i_s(t)$) with zero mean. The autocorrelation of $i_s(t)$ will
therefore be

$$R_i(t_1,t_2) = e\ \langle g\ \rangle\lambda(t_1)\delta\ (t_1 - t_2) \tag{4.10}$$

$\langle i_s(t)\rangle$ is given by $\langle i_s(t)\rangle = \frac{\eta}{h\gamma}\ e\langle g\rangle p(t) + e\langle g\rangle \lambda_o$

The spectral demities of $i_b(t)$, $i_A(t)$, and $e_A(t)$, given
by S , S_A, S_E are

$$S_b = \frac{2k\Theta}{R_b} \; ; \; S_A = \frac{2k\Theta}{R_A} \; ; \; S_E = \frac{2k\Theta}{g_m}$$

where,

k = Boltzman constant, Joules/°K

Θ = Temperature in °K

g_m = Transconductance of the amplifier   mhos

We assume the amplifier gain to be high enough to make any subsequent noise additions negligible. Let ℓ be the statistic we obtain by sampling the correlator output at the end of each baud T.

$$\therefore \; \ell = \int_0^T v_0(t)a_1(t)dt$$

$$= A \int_0^T [(\langle i_s(t)\rangle + i_b(t) + i_A(t) + i_S(t))R + e_A(t)]a_1(t)dt$$

$$\tag{4.11}$$

$$= (\ell_s + \ell_b + \ell_a + \ell_{ns} + \ell_w)$$

where

$$\ell_s = AR \int_0^T \langle i_s(t)\rangle a_1(t)dt \quad - \text{'signal' component}$$

$$\ell_{b/a} = AR \int_0^T i_{b/a}(t)a_1(t)dt \quad - \text{'Gaussian Noise' components.}$$
In this case they also are white.

$$\ell_{ns} = AR \int_0^T i_s(t)a_1(t)dt \quad - \text{Shot noise component}$$

$$\ell_w = A \int_0^T e_A(t)a_1(t)dt \quad - \text{'White Noise' component.}$$

We now find the square of the mean and variance of 'ℓ' and take their ratio to get the 'Signal to Noise Ratio' i.e. we are assuming the statistic to be Gaussian random variable. Such an assumption makes the performance calculation simple and allows us to see how the performance depends on various parameters [15]. In ordinary binary data transmission over fiber optic links with added Gaussian noise at receiver, such an assumption predicted the signal power required reasonably, close to the value found by exact calculations [15],[23]. We rely on this and go ahead and see whether any of the additional features of SSMA make this assumption more valid. In addition we assume that both shot noise and thermal noises are independent of each other and also the shot noise to be independent of the signal component $\langle i_s(t) \rangle$. Such an assumption is normally made with the SNR calculations. Therefore,

i) $\lambda_s = AR \int_0^T (\frac{\eta}{h\gamma} e\langle g \rangle p(t) + e\langle g \rangle \lambda_0) a_1(t) dt$

$$= AR\, e\langle g \rangle \frac{\eta}{h\gamma} \int_0^T \frac{b_E}{T} (K + \sum_{i=1}^{K} d_i(t - \tau_i) a_1(t - \tau_i))$$

$$a_1(t) dt + AR\, e\langle g \rangle \lambda_0 \int_0^T a_1(t) dt \qquad (4.12)$$

we have

$$\int_0^T a_1(t) dt = C/N.T$$

where

C = average of value of the (sum of all binary chips)
PN sequence. For M-sequences $C = 1$, and for Gold
sequence, $C = 2^{(n+1)/2}-1$, or -1 or, $-(2^{(n+1)/2}+1)$

where the sequence length $N = 2^n-1$, n odd.

$$\ell_s = AR\, e\langle g\rangle\, e\, \frac{\eta}{h\gamma} \cdot \frac{b_E}{T} \cdot \frac{KCT}{N} + \frac{\eta}{h\gamma}\, AR\, e\, \langle g\rangle\, \frac{b_E}{T}$$

$$\int_0^T [a_1(t)d_1(t) + \sum_{i=2}^K d_i(t-\tau_i)a_i(t-\tau_i)]\, a_i(t)dt$$

$$+ e\langle g\rangle\, AR\, \lambda_o \cdot CT/N$$

Usually λ_o is 10% of the signal intensity. Since now it is
divided by N its effect will be negligible

$$\ell_s = AR\, \frac{\eta}{h\gamma}\, e\langle g\rangle b_E \cdot KC/N + \frac{\eta}{h\gamma}\, AR\, e\langle g\rangle\, \frac{b_E}{T}$$

$$\left[\int_0^T d_1(t)a_1^2(t)dt + \int_0^T a_1(t)\left\{ \sum_i d_i(t-\tau_i)a_i(t-\tau_i)\ dt\right] \right.$$

$$= A'b_E KC/N + A'b_E[d_{1,o} + \frac{1}{T}\sum_{i=2}^K \left\{ d_{i,-1} \int_0^{\tau_i} a_i(t-\tau_i)a_1(t)dt \right. +$$

$$\left. d_{i,o} \int_{\tau_i}^T a_i(t-\tau_i)a_1(t)dt \right\}] \qquad (4.13)$$

Since

$$\int_0^T a_1^2(t)dt = T \ . \quad A' = \frac{\eta}{h\gamma}\, AR \cdot \langle g\rangle$$

The first and the second terms in brackets indicate the signal
and interference from   other users respectively.
As far as the bit energy b_E is concerned, both signal and
interference are weighted by the same value. So increasing
b_E does not increase performance from Multiple Access inter-
ference point of view. We take care of the first term in
eq. (4.13) in the threshold setting (as it is a constant term for
each correlator). The 2nd and third term appear as again
signal and noise terms i.e.

i.e. $\mathcal{L}_s = A' b_E d_{1,o} + A' b_E \cdot \frac{1}{T} \sum_i' d_{i,-1} R_{i,1}(\tau_i) + d_{i,o} \hat{R}_{i,1}(\tau_i)$

$$= A' b_E [d_{1,o} + \sum_i I_i(d_i, \tau_i)] \qquad (4.14)$$

The interference term $I_i(d_i, \tau_i)$ is familiar to us in Chapter 3
where the mean and variance of it are given. The variance is
given in eq. (3.13)

$$E[\mathcal{L}_s | d_{1,o}] = A' b_E d_{1,o} \qquad (4.15)$$

Since $I_i(d_i, \tau_i)$ has zero mean and

$$\text{Var}[\mathcal{L}_s] = (A')^2 b_E^2 \sum_{i=2}^{K} \sigma_{i,1}^2 \qquad (4.16)$$

ii) $\mathcal{L}_{ns} = AR \int_0^T i_s(t) a_i(t) dt$

$E[\mathcal{L}_{ns}] = 0$ by our zero mean assumption

$$\text{Var } [\ell_{ns}] = A^2 R^2 \int_0^T \int_0^T R_i(t_1, t_2) a_1(t_1) a_1(t_2) dt_1 dt_2$$

$$= A^2 R^2 e^2 \langle g^2 \rangle \frac{\eta}{h\gamma} \frac{b_E}{T} \int_0^T \int_0^T p(t_1) \delta(t_1 - t_2),$$

$$a_1(t_1) a_1(t_2) dt_1 dt_2 \quad \text{by eq.(4.10)}$$

$$= A^2 R^2 e^2 \langle g^2 \rangle \frac{\eta}{h\gamma} \frac{b_E}{T} \int_0^T p(t_1) a_1^2(t_1) dt_1$$

$$= A^2 R^2 e^2 \langle g^2 \rangle \frac{\eta}{h\gamma} \frac{b_E}{T} \int_0^T (K + \sum_{i=1}^K d_i(t - \tau_i) a_i(t - \tau_i)) dt$$

$$\tag{4.17}$$

$$a_1^2(t) = 1, \quad t\varepsilon(o, T)$$

Thus SS modulation does not have an additional advantage over other schemes in limiting the shot noise power. This is due to the fact that this shot noise is also white except for its non-stationarity and that SS modulation does not offer any advantage with white noise. Proceeding with the above

$$\text{Var } [\ell_{ns}] = A^2 R^2 e^2 \langle g^2 \rangle \frac{\eta}{h\gamma} \frac{b_E}{T} (KT + d_{1,o} \int_0^T a_1(t) dt$$

$$+ \sum_{i=2}^K \left\{ d_{i,-1} \int_0^T a_i(t - \tau_i) dt + d_{i,o} \int_i^T a_i(t - \tau_i) dt \right\})$$

$$\tag{4.18}$$

Thus the variance of the shot noise term depends on all the other user data bits $(d_{i,-1}, d_{i,o})$. Our approach is to consider its worst case value. Since for either M-sequences or Gold Sequences the maximum average value is always -ve (-1 for M-sequences) we can assume $d_{i,-1} = d_{i,o} = -1$ for all $i \neq 1$. This makes

$$\text{Var } [\ell_{ns}] = A^2 R^2 e^2 \langle g^2 \rangle \frac{\eta}{h\gamma} \frac{b_E}{T} (KT + d_{1,o} \frac{CT}{N} + \sum_{i=2}^{K}$$

$$- \int_{o}^{T} a_i(t - \tau_i) dt)$$

$$= A'' b_E(K + d_{1,o} \frac{C_1}{N} + \frac{1}{N} \sum_{i=2}^{K} C_i) \qquad (4.19)$$

where,

$$A'' = A^2 R^2 e^2 \langle g^2 \rangle \frac{\eta}{h\gamma} ,$$

C_i - average value of ith sequence

Since $C_1/N \ll 1$ we remove the explicit dependence of $\text{Var}[\ell_{ns}]$ on $d_{1,o}$ (essentially same for $d_{1,o} = +1$ or -1) and assume it to be -1. In addition we assume $C_1 = C_2 = C_K = C$ which is the worst case value in M-sequences or Gold sequences. Therefore,

$$\text{Var } [\ell_{ns}] = A'' b_E(K + KC/N) \qquad (4.20)$$

Worst case C/N is 6% for Gold sequences (and much less for M-sequences) and so the fractional increase (or change) of Var $[\ell_{ns}]$ is relatively small due to the above approximations.

iii) If we let $\ell_g = \ell_a + \ell_b = AR \int_0^T (i_b(t)+i_A(t))a_1(t)dt$

$$E[\ell_g] = 0$$

$$\text{Var } [\ell_g] = \text{Var } [\ell_a^2] + \text{Var } [\ell_b^2]$$

$$[\quad i_A(t),\ i_b(t) \text{ are independent}]$$

$$= A^2R^2 \int_0^T \int_0^T R_a(t_1,t_2)a_1(t_1)a_1(t_2)dt_1dt_2$$

$$+ A^2R^2 \int_0^T \int_0^T R_b(t_1,t_2)a_1(t_1)a_1(t_2)dt_1dt_2$$

$$= A^2R^2[\int_0^T \int_0^T S_A \delta(t_1-t_2)a_1(t_1)a_1(t_2)dt_1dt_2 \qquad (4.21)$$

$$+ \int_0^T \int_0^T S_b \delta(t_1-t_2)a_1(t_1)a_1(t_2)dt_1dt_2]$$

$$= A^2R^2T (S_A + S_b) \quad \because \int_0^T a_1^2(t)dt = T$$

$$= A^2 R^2T (\frac{2k\Theta}{R_A} + \frac{2k\Theta}{R_b}) = \frac{2k\Theta}{R} \cdot A^2R^2T \qquad (4.22)$$

Here we observe that as R_A and R_B increase variance of ℓ due to Gaussian noise decreases. This is where the deliberate

introduction of ISI is made at the receiver to reduce thermal noise effect, by increasing R_A and R_b (or equivalently R).

Before doing such a thing, we continue now with our analysis.

iv) $\ell_w = A \int_0^T e_A(t) a_1(t) dt$

$E[\ell_w] = 0$

$$Var \ [\ell_w] = A^2 \int_0^T \int_0^T S_E \ \delta(t_1-t_2) a_1(t_1) a_1(t_2) dt_1 dt_2$$

$$= A^2 T \cdot \frac{2k\Theta}{g_m} \tag{4.23}$$

Thus by eqs. (4.16), (4.20), (4.22) and (4.23)

$$Var \ [\ell] = Var \ [\ell_s] + Var \ [\ell_{ns}] + Var[\ell_g] + Var[\ell_w]$$

$$= (A')^2 b_E^2 \sum_{i=2}^K \sigma_{i,1}^2 + A'' b_E (K + \frac{KC}{N}) +$$

$$A^2 R^2 T \cdot \frac{2k\Theta}{R} + A^2 T \cdot \frac{2k\Theta}{g_m} \tag{4.24}$$

$$E^2[\ell] = E^2[\ell_s] = (A')^2 b_E^2 \tag{4.25}$$

$$SNR = \frac{E^2[\ell]}{var[\ell]} = \frac{(A')^2 b_E^2}{(A')^2 b_E^2 \sum_{i=2}^K \sigma_{i,1}^2 + A'' b_E (k+KC/N) + A^2 R^2 T \cdot \frac{2k\Theta}{R} + A^2 T \cdot \frac{2k\Theta}{g_m}}$$

$$\tag{4.26}$$

$$= \frac{1}{\sum_{i=2}^{K} \sigma_{i,1}^2 + \frac{A''}{(A')^2 b_E}(K+KC/N) + \frac{2k\Theta \cdot A^2 R^2 T}{(A')^2 b_E^2}(1/R+\bar{R}^2/g_m)}$$

Thus it is seen as b_E ('bit energy') increases shot noise and thermal noise effects reduce (latter's more rapidly). Also as R increases the effect of $e_b(t)$ also reduces as seen in the denominator. Beyond a certain value, any increase in b_E does not improve the performance as the effect of interference is unaltered with b_E. That is the performance 'levels off' after a certain b_E, which depends only on the cross correlations of the individual PN-sequences. The greater the number of users, the larger is the shot noise. We observe later that this effect is small compared to the interference from other users directly.

Substituting for A', A''

$$SNR = \frac{1}{\sum_{i=2}^{K} \sigma_{i,1}^2 + (\frac{h\gamma}{\eta}) \frac{\langle g^2 \rangle}{\langle g \rangle^2} \cdot \frac{1}{b_E}(K+ \frac{KC}{N}) + (\frac{h\gamma}{\eta})^2 \cdot \frac{2k\Theta T}{e^2 \langle g \rangle^2} \cdot \frac{1}{b_E^2}}$$
$$(1/R+R^{-2}/g_m) \qquad (4.27)$$

The use of APD with mean gain $\langle g \rangle$ is explicit now. $\langle g^2 \rangle$ and $\langle g \rangle$ are related by

$$\langle g^2 \rangle = [k_1 \langle g \rangle + (2- \frac{1}{\langle g \rangle})(1-k_1)]\langle g \rangle^2$$
$$= (k_1-1)\langle g \rangle + 2(1-k_1)\langle g \rangle^2 + k_1 \langle g \rangle^3 \qquad (4.28)$$

where k_1 is the ionization ratio of the photodiode. For silicon diodes k_1 is 0.01 to 0.1 (smaller the better) and for Ge diode it is approximately 0.5. The thermal noise decreases with increasing APD gain and hence the performance improves. However this is not monotonic because increasing $\langle g \rangle$ increases the shot noise and so after a certain value of $\langle g \rangle$ the total noise increases with increasing $\langle g \rangle$ and performance falls down. By letting the total noise dependent on $\langle g \rangle$ equal to N_T, we can optimize $\langle g \rangle$ to have N_T take its minimum value. Therefore,

$$N_T = \frac{h\gamma}{\eta} \frac{\langle g^2 \rangle}{\langle g \rangle^2} \frac{1}{b_E}(K + \frac{KC}{N}) + (\frac{h\gamma}{\eta})^2 \frac{2k\Theta T}{e^2\langle g \rangle^2} \cdot \frac{1}{b_E^2}(1/R + R^{-2}/g_m)$$

$$(4.29)$$

$$= \frac{h\gamma}{\eta}(k_1\langle g \rangle + (2 - \frac{1}{\langle g \rangle})(1-k_1)) \frac{1}{b_E}(K + \frac{KC}{N}) + (\frac{h\gamma}{\eta})^2 \frac{2k\Theta T}{e^2\langle g \rangle^2}$$

$$\frac{1}{b_E^2}(1/R + R^{-2}/g_m)$$

letting $G = \langle g \rangle$

$$N_T = A_1(k_1 G + (2 - \frac{1}{G})(1-k_1)) + A_2 \cdot \frac{1}{G^2}$$

where,

$$A_1 = \frac{h\gamma}{\eta} \cdot \frac{1}{b_E}(K + \frac{KC}{N})$$

$$A_2 = (\frac{h\gamma}{\eta})^2 \cdot \frac{2k\Theta T}{e^2 b_E^2} \cdot (1/R + R^{-2}/g_m)$$

differentiating w.r.t. G and setting the result to zero
we have

$$\frac{dN_I}{d_a} = A_1[k_1+(1-k_1) \cdot \frac{1}{G^2}] - \frac{2A_2}{G^3} = 0$$

or

$$A_1 K_1 G^3 + A_1(1-k_1)G - 2A_2 = 0 \qquad (4.30)$$

The solution of the equation (4.30) provides us with the
optimum gain $\langle g \rangle$ opt.

In digital communication systems, the accepted
performance criterion is probability of bit error. We
obtain it simply due to our assumption of $\mathcal{L}$ as Gauss. random
variable, as

$$P_e = \text{erfc}_* \ (\text{SNR}^{1/2}) \qquad (4.31)$$

where,

$$\text{erfc}_* (x) = \frac{1}{\sqrt{2\pi}} \int_x^\infty e^{-t^2/2} \ dt$$

We give the results of this criterion in the next
chapter where we observe the variation of P_e with b_E, K,
$\langle g \rangle$, N and R. The variations due to the last parameter, R
motivates us to consider the case of ISI introduction by
having a high value of R. We consider $\wedge$ this case in the
next section.

4.2 BANDWIDTH LIMITATION AT THE RECEIVER:

As we saw, the bandwidth limitation at the receiver is caused by introducing a high impedance front end after the photodetector. Such a thing causes the data pulses to overlap and to introduce inter symbol interference. This problem, namely that of bandwidth limitation can even be generalized to the fiber channel also, in which case the pulses get overlapped in the optical format itself before arriving at the receiver. Such a condition is as shown in Figure 4.3.
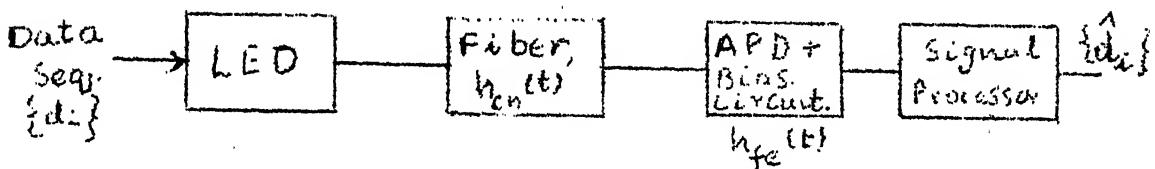
Fig. 4.3

The optical intensity $\lambda(t)$ at the input to APD is now modified as

$$\lambda(t) = \frac{\eta}{h\gamma} \frac{b_E}{T} (K + \sum_i d_i(t-\tau_i)a_i(t-\tau_i) * h_{ch}(t) \qquad (4.32)$$

and, average value of the shot noise at the output of amp. is

$$v_o(t) = \frac{\eta}{h\gamma} \frac{b_E}{T} (K + \sum_i d_i(t-\tau_i)a_i(t-\tau_i)) * h_{ch}(t) * h_{fe}(t)$$

$$= \frac{\eta}{h\gamma} \frac{b_E}{T} (K + \sum_i d_i(t-\tau_i)a_i(t-\tau_i)) * h_1(t)$$

where $h_1(t) = h_{ch}(t) * h_{fe}(t)$ is the equivalent base band channel impulse response.

Now how to process the detected electric (composite) signal to decide on $d_1(t)$? One approach is to take up the Gaussian noise method where in the signal is distored by additive white Gaussian noise and Inter-symbol interference [29]. The interference from other users and the shot noise can be approximated as Additive and Gaussian. The other is to optimally process the detected signal with associated shot noise, AWGN and ISI [8]. However, for reasons explained in Chapters 2 and 3, we tend to choose the suboptimum receiver. Thus we have taken up the first method where only a signal embedded in white noise is received after distored by ISI. So we proposed the matched filter equalizer structure for the problem at hand. It is as shown in Fig. 4.4, i.e. we use matched filter-decision feedback equalizer structure to decide on $d_1(t)$ and obtain its performance. But such an approach immediately warns of the low signal to noise ratio obtained at the O/P of the matched filter. The low SNR is due to the fact that all the SS modulated data sequences passed through the band limited channel by which they are severely distored and the cross correlations of which are no more small but same as the order of the autocorrelations of themselves. In view of Chapter 3, this can be explained as follows. There we
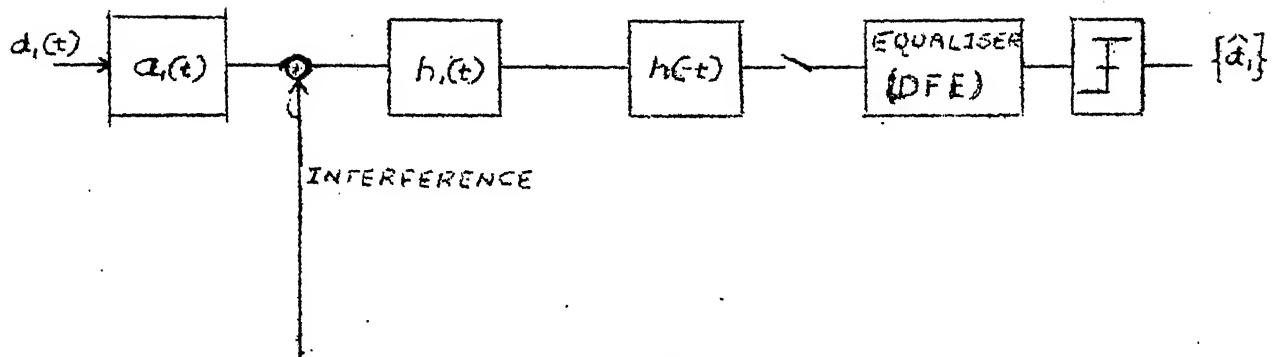
$$h(t) = h_1(t) * a_1(t)$$
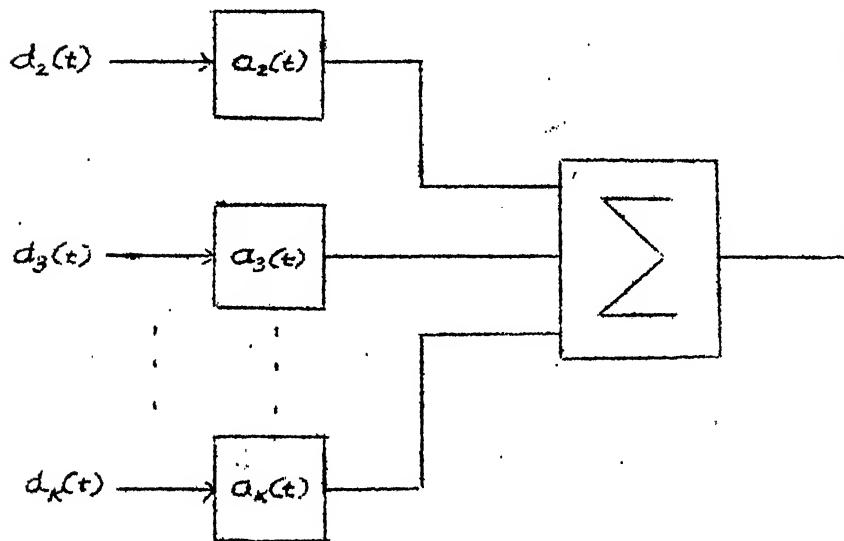
Fig 4.4: Matched filter - DFE Receiver

Table 4.1

R = 500KΩ   C = 10 pF   N = 511

	Autocorrelation	Cross Correlation	SNR
ISI Present	0.2314E-02	0.5698E-03	4.06
ISI Absent	0.1562E-04	0.3057E-07	520

have shown that the cross correlation of two sequences is
dependent upon their autocorrelations. The PN sequences, being
Pseudo random have a very small autocorrelation outside the
chip interval. Thus their cross correlations are also small.
But now the PN sequences are so much spread that their auto-
correlations will not be any more near-impulsive. Hence the
cross correlations also will not be small. And in this low
SNR environment the performance of DFE is very poor. So such
a structure cannot perform satisfactorily. For illustration
we have shown in Table 1 autocorrelation and the correlation
values of a PN sequence with another PN sequence with and
without bandlimitation. The resulting low SNR is as expected
above. This is infact the reason, historically, for using
SSMA only on a channel with available bandwidth [24]. Otherwise,
the spreading of the data or N has to be decreased accordingly.
Infact, it is for the same low SNR reason, that chip level
detection of sequences is not done in SSMA.

So, to solve the problem at least partially, without
losing the advantage we saw with high impedance front end. We
took the following path. We assumed that the fiber does not
introduce any ISI. The possible ISI is only caused by the
high imp. front end. For convenience we repeat the receiver
block diagram in Fig. 4.5.
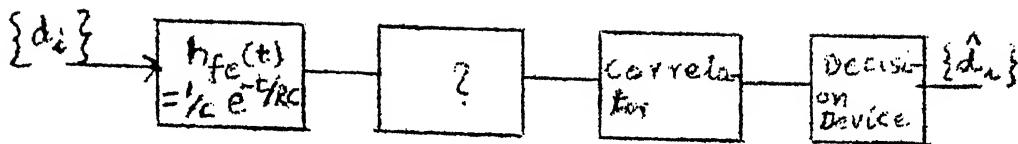
Fig. 4.5: SSMA in band limited case

Since, we already chose the correlator for the SSMA case we retain it as it is. Now to make the SNR high at the output of the correlator we need to nullify the adverse effect of the $h_{fe}(t)$ but retain the advantage with high R. From the frequency domain point of view it is clear that $h_{fe}(t)$ alternates the high frequency components. So the simplest solution will be to follow it up with an inverse filter which accentuates the high frequencies. To make it explicit we seperate $h_{fe}(t)$ into cascade of two units and put an inverse filter to the second one. It is as shown in Figure 4.6.
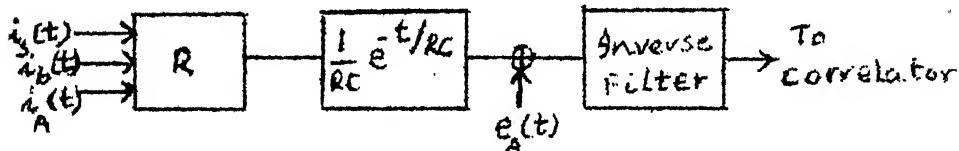
Fig. 4.6: Inverse filter solution

The Fourier transform of $\frac{1}{RC} e^{-1/RC} = \frac{1}{RCj\omega+1}$ $\qquad$ (4.33)

We choose F.T. of the Inverse filter impulse response to be $(RCj\omega+1)$ such that the cascade of the two filters produces an impulse response of $R\,\delta(t)$. Physically the inverse filter is the direct addition of the output of $h_{fe}(t)$ with a differentiated and amplified version of itself. Thus at the output of the inverse filter (or at imput to the correlator) the filtered versions of shot noise (including signal) and thermal noises $i_A(t)$ and $i_b(t)$ are spectrally restored back to their original shapes. So the analysis of the unlimited bandwidth case is directly applicable. However, the white noise source $e_A(t)$ is affected by the inverse filter rather harmfully. In frequency domain, the $e_A(t)$ with a constant p.s.d. of S_E is now modified by as

$$S_{OE} = S_E \cdot |H_{inv}(f)|^2 = S_E(R^2C^2\omega^2+1) = \frac{2k\Theta}{g_m}(R^2C^2\omega^2+1)$$

$$(4.34)$$

Its autocorrelation function is given by

$$R_e(\tau) = \frac{2k\Theta}{g_m}\left(\delta(t) - R^2C^2\frac{d^2}{d^2}\delta(\tau)\right) \qquad (4.35)$$

If we let $e_0(t)$ be the Gaussian noise corresponding to $e_A(t)$ and $\mathcal{l}_{o\omega}$, the statistic contribution due to it

$$\mathcal{l}_{o\omega} = \int_0^T e_0(t)a_1(t)dt$$

$$E[\mathcal{l}_{o\omega}] = 0$$

$$\text{Var}[\ell_{o\omega}] = \int_o^T \int_o^T R_e(\gamma) a_1(t_1) a_1(t_2) dt_1 dt_2 = \frac{2k\Theta}{g_m} \Big[$$

$$\int_o^T \int_o^T \delta(t_1-t_2) a_1(t_1) a_1(t_2) dt_1 dt_2 + \int_o^T \int_o^T$$

$$+ R^2 C^2 \frac{d^2(\delta(t_1-t_2))}{dt_1 dt_2} a_1(t_1) a_1(t_2) dt_1 dt_2 \Big]$$

$$= \frac{2k\Theta}{g_m} (T + R^2 C^2 \cdot \int_o^T \int_o^T \frac{d^2(\delta(t_1-t_2))}{dt_1 dt_2} \cdot$$

$$a_1(t_1) a_1(t_2) dt_1 dt_2) \qquad (4.36)$$

We compare this with the variance of $(i_b(t)+i_A(t))$, given in eq. (4.22).

$$\text{Var} [\ell_g] = 2k\Theta RT$$

Since $R \gg 1/g_m$ (normally, otherwise we would not have considered the inverse filter at all), the first term can be neglected. If

$$T \gg \frac{RC^2}{g_m} \int_o^T \int_o^T \frac{d^2\delta(t_1-t_2)}{dt_1 dt_2} a_1(t_1) a_1(t_2) dt_1 dt_2$$

$$(4.37)$$

We can neglect this term. However if T is only of the order of the right hand side, we may not neglect this but approximate it as nearly $2K\Theta RT$. So now the net contribution due to thermal noise is

$$\text{Var} [\ell_g] = 2K\Theta RT \times 2 = 4K\Theta RT \qquad (4.38)$$

This increase in thermal noise can be taken care of by
modifying $\langle g \rangle_{opt}$. The decrease in the total thermal noise
power due to high R is still present inspite of the doubling
of $Var[l_g]$. We can see this more clearly by making an
analysis in frequency domain.

The power spectral density of $e_{th}(t)$ (due to $i_b(t)$
and $i_A(t)$) at the output the inverse filter $S_{th} = \frac{2k\Theta}{R} \cdot R^2$

$$= 2k\Theta R$$

The power spectral density of $e_o(t)$ (due
to $e_A(t)$ at the output the inverse filter $S_{oE} = \frac{2k\Theta}{g_m} \cdot (R^2 C^2 \omega^2 + 1)$
where $\omega = 2\pi f$.

These are as shown in Fig. 4.7.
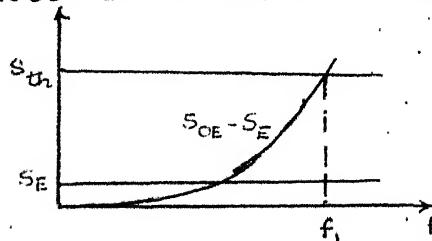
Fig. 4.7: p.s.d of $e_{th}(t)$ and $e_o(t)$

The total thermal noise p.s.d. is

$$S_T = S_{th} + S_{oE} = 2k\Theta R \left(1 + \frac{1}{g_m R} + \frac{RC^2 \omega^2}{g_m}\right) \qquad (4.39)$$

$$S_T = S_{th} + S_{oE} = 2k\Theta R \left(1 + \frac{RC^2 \omega^2}{g_m}\right)$$

If the bandwidth of the data signal is approximately 1/T then
the Bandwidth of the SS modulated signal is N/T. So for

the second term to be small compared with 1 (i.e. if we want f_1 to be equal to N/T)

$$\frac{RC^2\omega^2}{g_m} \Big|_{\omega = \frac{2\pi N}{T}} < 1$$

i.e.

$$\frac{RC^2(2\pi N/T)^2}{g_m} < 1 \text{ or } T > \sqrt{R/g_m} \cdot 2\pi NC \tag{4.40}$$

if $T = \sqrt{R/g_m} \cdot 2\pi NC$, then S_{oE} will be still less than S_{th} but of the same order of magnitude as that of S_{th}. As an alternative if we consider T to be such that both powers in S_{th} and S_ω to be equal. Then,

$$\frac{N}{T} = \int_0^{N/T} \frac{RC^2}{g_m} \omega^2 df = \frac{RC^2}{g_m} \cdot 4\pi^2 \cdot \frac{f^3}{3}\Big|_0^{N/T} = \frac{RC^2}{g_m} \cdot \frac{4\pi^2}{3} \cdot \left(\frac{N}{T}\right)^3$$

or,

$$\left(\frac{T}{N}\right) = \frac{RC^2}{g_m} \cdot \frac{4\pi^2}{3} \text{ i.e. } T = \sqrt{R/g_m} \cdot \frac{2\pi NC}{\sqrt{3}} \tag{4.41}$$

resulting in a smaller value of T.

To ensure that this equality of S_{th} and S is maintained at the O/P of the correlator also, we can choose the inverse filter characteristic such that it passes the signal frequency of interest only i.e. above $f = N/T$ it attenuates the noises completely.

Thus the receiver proposed solves the problem partially. The performance can again be found by assuming ℓ to be Gauss. r.v. Hence,

$$P_e = \text{erfc}_*(\text{SNR}^{1/2})$$

where the SNR now is slightly degraded than the first case.
The variations of P_e with optical power, $\langle g \rangle$, R,N are same as
before (Chapter 5). The limitation of this receiver is in the
last approximation we made regarding the noise contribution
due to $e_A(t)$. For an amplifier with low S_E only this is
valid, otherwise not. Also arbitrarily large N is not
possible due to the fact the p.s.d. of $e_o(t)$ increases as
square of frequency and at higher values of frequency it tends
to be infinite, where upon the approximation will no more be
valid.

4.3 SIMULATION:

The system considered in Section 4.1 is simulated on
DEC-10. The details of the simulation are given in Appendix B.
The results are presented in Chapter 5. The simulations are
done for no APD gain (i.e. $\langle g \rangle = 1$) since the probability
density function of it is quite complex.

CHAPTER 5

PERFORMANCE RESULTS AND CONCLUSIONS

This chapter begins with the presentation of the
theoretical performance results for the receivers proposed
in Chapter 4. The results are then interpreted and compared
with results obtained by simulation . We then give a critical
evaluation of the proposed system giving its merits and
limitations. It concludes with some suggestions for further
work.

5.1 NUMERICAL RESULTS ON THEORETICAL PERFORMANCE:

As mentioned in Chapter 4, we take the performance
criterion to be the probability of bit error given in terms
of the signal to noise ratio SNR in eq. (4.27).

Case I: Unlimited bandwidth availability:

For convenience, we repeat here the expressions for
the signal to noise ratio (SNR) and probability of error.

$$P_e = erfc_*(SNR^{1/2})$$

$$SNR = \frac{1.0}{\sum_{i=2}^{K} \sigma_{i,1}^2 + (\frac{h\gamma}{\eta})[k_1 \langle g \rangle + (2 - \frac{1}{\langle g \rangle})(1-k_1)]\langle g \rangle^2 \frac{1}{b_E}(K + \frac{KC}{N}) + (\frac{h\gamma}{\eta})^2 \cdot \frac{2k\Theta T}{e^2 \langle g \rangle^2} \cdot \frac{1}{b_E^2}(1/R + R^{-2}/g_m)}$$

Where all the symbols are as explained earlier. To get numerical results, we fix values for some of these symbols. We choose k_1 to 0.1 assuming a silicon detector (for Germanium, K 0.5). Θ is chosen to be 300°K and the data symbol duration T is taken to be 1.562×10^{-5} sec. This corresponds to data rate of 64K bps, typical of a digitized voice channel with 8 bit PCM. Use of ADM etc. can accomodate upto 2 voice channels in this data rate. Or it can even be a time multiplexed low data signals emanating from a user source of information. The amplifier transconductance g_m is taken to be $4m\mho$. The constants are

$$h\gamma/\eta = 3.117 \times 10^{-19} J, \quad k = 1.37 \times 10^{-23} J/^{\circ}K, \quad e = 1.602 \times 10^{-19} \text{ coloumb.}$$

We have considered two cases of N=511 and 1023. The average value (worst case) C is dependent on the type of PN sequence and the code sequence length, N. Since M-sequences available for the above code lengths are only 24 and 30 respectively. We did not consider them. However for comparison sake the multiple access interference term $\sum_{i \neq 1}^{K} \sigma_{i,1}^2$, for K = 20 is tabulated in Table 5.1 for both M-sequences and Gold sequences. The Gold sequences are considered for their large set of 513 and 1025 sequences for N=511 and 1023 respectively. For these code sequence lengths the worst case is such that C/N is approximately 6%. We vary

the other parameters over a set values to observe the variation of the probability of bit error, P_e. We first vary the photodetector (APD) gain and calculate the P_e. This is done for varying optical power p as well as varying K, the number of users. The variations are also observed with varying R, the equivalent bias resistance (from here onwards referred to as bias resistance) and with both cases of N=511 and 1023. The data of these are given in Tables 5.2-5.7 and the plots are given in Figs. 5.1 to 5.6 where each figure corresponds to a specific N, and R. In all these cases we observe the performance first improving then saturating, and finally deteriorating with increasing APD gain.

We then evaluate the probability of error with varying optical power, again for certain values of K and for both values of N. The associated APD gains are chosen to be optimum such that the P_e is minimum for that value of optical power. These gains are obtained by solving eq. (4.30) for each value of p. These variations are also observed with different R. The data are given in Tables 5.8 and 5.9 and the plots in Figs. 5.7 and 5.8. We then give the important variations of P_e with K, the number of users in multiple access environment, again with optimum gains at chosen optical powers. This data is presented in Tables 5.10 and 5.11 and plotted in Figs. 5.9 and 5.10. We finally present the

data in Table 5.12 and 5.13 of P_e versus R for unit and optimal APD gains. The plots are given in Figs. 5.11 and 5.12.

In the above case we assumed unlimited bandwidth at the receiver. But this is not so for high values of R due to non-zero capacitance values. For this problem the front end circuit is followed up by an inverse filter such that the signals are 'whitened' as given in Chapter 4.

The analysis of Section 2 of Chapter 4 indicates that R,C,N, g_m should be such that the condition in eq. (4.40 or 4.41) is satisfied for a given T to make the noise enhancement due to inverse filter small. However, T can be smaller than this resulting in a higher contribution from S_ω but still keeping the total thermal noise contribution less than what would have been obtained by keeping a low value of R in order to avoid the bandwidth limitations. As an illustration we consider both the situations.

1. $R = 1\,\Omega$ hence no ISI

At the output of the amplifier total thermal noise spectral density (normalized by R^2) = $2k\theta/R\,(1+ 1/g_m R^2)$

$\qquad S_T = 201 \times 2k\theta$ for $g_m = 5$ m℧

2. $R = 500\,K\Omega$ and $C = 10^{-11}F$ hence ISI is present.

At the output of the inverse filter, total thermal noise p.s.d.

$$= \frac{2k\theta}{R} + \frac{2k\theta}{g_m} \cdot R^{-2} + R^{-2} \cdot R^2 C^2 \omega^2 \cdot \frac{2k\theta}{g_m}$$

$$= \frac{2k\theta}{R} \left(1 + \frac{1}{g_m R} + \frac{RC^2 \cdot \omega^2}{g_m} \right)$$

$$= 2k\theta \left(1/R + 1/g_m R^2 + \frac{C^2 \cdot (2\pi N/T)^2}{g_m} \right) \text{ at } f = N/T$$

$$= 2k\theta \times 8.4 \times 10^{-4}$$

Thus introducing deliberate ISI by a high impedance front end, gives a considerably high performance over that obtained by low R front end circuit, even though there is enhancement of noise due to inverse filter.

But for the above modifications of the net thermal noise power, the system performance depends essentially the same way as it does in the first case. Due to the increase in this thermal noise power the performance slightly degrades at low optical powers. Thus it is appropriate to interprete the results of the previous case first and then see the changes required to get suitable performance in the present case. In the next section we try to interprete the results obtained with unlimited bandwidth case and compare them with the simulation results obtained.

5.2 INTERPRETATION OF THE PERFORMANCE RESULTS:

First, we go through the variation of P_e with APD gain. From Figs. 5.1 to 5.6, we see that

1. The probability of error decreases first, then flattens, and finally increases, with increasing APD gain. This is so because of the fact (as given in eqn. 4.29) that the sum of shot noise and thermal noise decreases first with increasing APD gain. Thus the performance improves. But at medium gains the variance of the gain tends to be such that the decrease in thermal noise is compensated by an increase in the shot noise which tend to cancel out and performance remains constant. Further increase of the gain results in more shot noise contribution than thermal noise reduction leading to the increase of the total noise resulting in increase of P_e. So there is an optimum value of <g> which minimizes the total noise which is found by solving eq. (4.30). This result is consistent with the single user case.

2. With increasing optical power the optimum gain decreases for a given number of users K. This is due to the reduced shot noise and thermal noise which is explicit in eq.(4.27). Thus a proper choice of the optical power has to be made to use as minimum APD gain as possible or even to do a way with the APD.

3. With increasing K the number of users, the optimum gain shifts left (or decreases). This is an important factor and is peculiar to the SSMA in fiber optic communication. This is due to the increase in number of users which results in a higher optical power (not that of signal) hence higher shot noise. unless the optical power is sufficiently high the shot noise power can exceed the multiple access power which normally exceeds the additive noise.

4. Finally increasing R has an important effect on the APD gain. We observe the $\langle g \rangle_{opt}$ decreases with increasing R. This is so because of the reduced thermal noise power due to increased R as we have seen earlier. Thus for R=1KΩ the optimum gain at p = 50 pW (for N=1023, K=50) is about 97 where the corresponding value at R=500KΩ is about 11 resulting in a performance difference of more than an order. Thus a proper choice of the bias resistance can obviate the need for a high gain APD.

Then by observing the probability of error vs. optical power in Figs. 5.7 and 5.8 we can conclude the following.

1. The probability of error is high at low optical power, falling off rapidly with increasing optical power. However such a decrease does not happen continuously. At high optical powers the effects of shot noise and thermal noise

tend to/negligible and the multiple access interference term
is dominant. Since this is independent of the optical power
the probability of error saturates at a value which is
'irreducible'. This value can only be improved by choosing
low cross correlation sequences and by taking a higher value
of N. With doubling N, the bandwidth required also gets
doubled. The use of an inverse filter is limited because
(as shown in the previous section) the thermal noise power
enhancement is proportional to N^2.

2. It is clear from these plots that an increase in R decreases
the required optical power, to achieve a certain error
rate   It is more at low optical powers. The decrease
is negligible at high powers due to the dominance of
multiple access interference over thermal noise. But the
low powers are only of interest to us where we can still
have reasonable performance, with proper value of R .
e.g. if the basic data signal with a rate of   64K bps
is a voice channel, an acceptable error rate will be 10^{-5}.
Thus at this value we see there is a decrease of the
required optical power by around factor of four in going
from a value of R of 1KΩ to 500KΩ. As mentioned earlier
these results are to be seen in light of the peak optical
power required. Thus at $P_e=10^{-5}$ we require the peak
optical power to be (for K=50, N=1023) 2xkxp which is

equal to 40 nW at R=1K and 10 nW at R=500K. Since the
saturation of the LED emitted optical powers can occur at
high drive currents, thus making the system performance
poor and making the relation between optical power and drive
current nonlinear, a high value of R will always be preferred
from this point of view.

We then observe the variation of the probability with
varying K at different optical powers with optimum APD
gains. At low optical powers the dependence of P_e on K is
less due to the thermal noise and shot noise dominance. However
still there will be an increase in P_e with increasing K
because the shot noise power increases linearly with K. At
high powers P_e increases with increasing K due to increased
multiple access interference. We have shown these cases for
N = 511 and 1023 in Figures 5.9 and 5.10. It is then with
increasing N the performance improves but at the expense of
increased bandwidth have shown only up to K equal to 100
because beyond this, the low performance obtained is not
generally acceptable.

We finally observe the variations of P_e with R. The
APD gain at these points are again chosen to be optimal. At
high optical power P_e is independent of R since the thermal
noise power at both low and high values of R is negligible
compared to the signal power. However at low powers, . ` e.g.

at p = 1 nW for N = 1023 we obtain a performance at R=500KΩ
three orders of magnitude better than that obtained at
R=10Ω . To get the performance of the former we need to
increase the power by about 5 dB at R=10Ω. Once again it is to be
noted, such an increase in optical power puts restrictions on
the linearity of the LED. Thus the use of high impedance
front end is justified at low optical powers.

These conclusions will also be true for the limited
bandwidth case but with slightly reduced performance. We also
performed simulation (details in Appendix B) for the
unlimited bandwidth case. Due to the complex   nature of
the APD gain probability density functions, we assumed unity
gain (or PIN diode) case. Due to the heavy   computation
time required, we performed the simulation only for a low
SNR case resulting in a theoretical P_e of 2.5×10^{-3} with
N=511, Using 10^3 iterations the observed probability of error
was about 1.5×10^{-2}. Such a discrepency could be due to the
Gaussian approximation for the decision statistic and due
to the independence assumption of shot noise on signal. From
these facts some additional conclusions can be made about
the receivers and the system as a whole. This is done in
the next section.

5.3 CONCLUSIONS AND SUGGESTIONS FOR FURTHER WORK:

Merits and Limitations of the Receiver:

The receivers in both the unlimited and limited bandwidth cases performed reasonably well at optical powers of practical feasibility. The particular problem of introduction of ISI is reasonably solved by the inverse filter. However, the net thermal noise reduction will only be smaller over that of the case where R is small when the code sequence lengths are of reasonable values. At very high code lengths the enhancement can be of the same order as or even more than that of the no ISI case. Then the use of high impedance front end is not of any use. The advantage we get at low values of code length is considerable from both the performance point of view as well as the less stringent requirement on the linear range of LED or Laser. As mentioned in [1] and observed here, in the asynchronous mode of operation, with SSMA, the number of new users with satisfactory performance is around N/10. In a synchronous case this number will be much better. But such a restriction is what is not preferred and is in fact the major reason for choosing SSMA in preference to TDMA. So essentially SSMA proves superior to TDMA, by its asynchronous operation when the available bandwidth is more than the required bandwidth. In data networks, this is usually so

and SSMA can prove to be effective over TDMA. However the increased shot noise power and high peak power requirement of driving LED are some disadvantages of SSMA.

The performance obtained by Gaussian approximation will be closer to the exact performance when

i) the signal to noise ratio is relatively high

ii) the number of asynchronous users is high which makes the multiple access interference tends to be Gaussian. Also the shot noise tends to be Gaussian when $\lambda(t)$ is high most of the time [25]. This will be true for our high number of users case.

iii) the APD gains are relatively low [23], which is also true in our case.

Suggestions for Further Work:

In this thesis we considered only the suboptimal receivers for reasons of their simplicity and satisfactory performance. Unlike this, an optimum receiver structure may be derived to process the composite signal. In the system considered here we made an important assumption of the existance of perfect synchronization between the transmitted and locally generated PN sequences not only at the chip level but at the frame level also. In SSMA, such a synchronization is difficult to obtain and sometimes the number of users can be limited by

the synchronization problem only [24] . So it needs to be analysed how the performance changes with lack of perfect synchronization.

The simulations are difficult to make for high data lengths due to the high CPU times required. A better way can be to implement the system to check the validity of the performance results presented here. For this case synchronization can be directly made between transmitter and receiver.

The case of unequal received powers of user signals, a case more realistic to SSMA is not considered here. However, such a situation can be considered which only modifies the multiple access interference.

Finally, we also made the assumption of distortionless fiber channels. Though this might be true for the code sequence lengths we considered, at higher values of N the dispersion effects of the fiber can be analysed. Also the assumption of ideal nature of the LED or Laser (linearity and spectral coherence) and photo diode can be relaxed and the non ideal case be analysed.

Table 5.1
Multiple Access Interference
N = 511   K = 20

M.A. Interference value, $\sigma_{i,1}^2 \times 10^3/2$

M—Sequences	Gold Sequences
0.665	0.641
0.657	0.640
0.653	0.718
0.673	0.662
0.643	0.716
0.680	0.678
0.663	0.726
0.665	0.607
0.633	0.671
0.659	0.662
0.673	0.684
0.640	0.659
0.660	0.694
0.668	0.644
0.643	0.653
0.641	0.652
0.642	0.681
0.656	0.676
0.690	0.698

Table 5.2
P_e vs. Versus APD gain

R = 1.0KΩ N = 511

APD gain	Probability of error, P_e			
	p = 200 pW		p = 1000 pW	
	K = 10	K = 20	K = 10	K = 20
1	.44856E+00	.44857E+00	.25952E+00	.26011E+00
5	.25960E+00	.26028E+00	.11855E-00	.21088E-02
10	.10076E+00	.10374E+00	.85783E-07	.43844E-05
15	.29664E-01	.33527E-01	.31438E-10	.12223E-06
20	.69708E-02	.96947E-02	.16339E-12	.19312E-07
25	.14088E-02	.27890E-02	.60600E-14	.73248E-08
30	.26623E-03	.87042E-03	.77737E-15	.43379E-08
35	.50914E-04	.31128E-03	.21411E-15	.32678E-08
40	.10521E-04	.10069E-03	.95122E-16	.28264E-08
45	.24635E-05	.64519E-04	.57474E-16	.26580E-08

Table 5.3

P_e Versus APD Gain

$R = 91 K\Omega$, $N = 511$

| APD gain | Probability of error (P_e) | | | | | |
| | p=200pW | | p = 500 pW | | p=100 pW | |
	K=10	K=20	K=10	K=20	K=10	K=20
1	.911E-01	.939E-01	.797E-03	.154E-02	.330E-07	.245E-05
5.	.734E-07	.571E-05	.336E-14	.615E-08	.304E-17	.756E-09
10	.114E-11	.896E-07	.177E-16	.177E-08	.623E-18	.537E-09
15	.327E-13	.408E-07	.863E-17	.172E-08	.593E-18	.576E-09
20	.130E-13	.410E-07	.947E-17	.202E-08	.712E-18	.651E-09
25	.133E-13	.522E-07	.131E-16	.245E-08	.911E-18	.744E-09
30	.199E-13	.719E-07	.197E-16	.313E-08	.119E-17	.853E-09
35	.347E-13	.101E-06	.306E-16	.394E-08	.157E-17	.979E-09
40	.647E-13	.144E-06	.480E-16	.495E-08	.207E-17	.112E-08
45	.123E-12	.203E-06	.754E-16	.620E-08	.273E-17	.128E-08

Table 5.4

P_e Versus APD gain

R = 500K Ω N = 511

APD gain	Probability of error, (P_e)				
	p=100pW K=10	p = 200 pW K=10	K=20	p = 1000 pW K=10	K=20
1	.597E-01	.144E-02	.252E-02	.242E-14	.375E-08
5	.131E-07	.641E-13	.267E-07	.389E-18	.434E-09
10	.462E-11	.932E-15	.126E-07	.357E-18	.472E-09
15	.120E-11	.585E-15	.165E-07	.464E-18	.545E-09
20	.163E-11	.167E-14	.250E-07	.621E-18	.631E-09
25	.350E-11	.372E-14	.385E-07	.836E-18	.729E-09
30	.850E-11	.849E-14	.588E-07	.112E-17	.841E-09
35	.208E-10	.191E-13	.883E-07	.150E-17	.969E-09
40	.493E-10	.418E-13	.130E-06	.200E-17	.111E-08
45	.111E-09	.886E-13	.188E-06	.266E-17	.127E-08

Table 5.5
P_e Versus APD gain
$R = 1K\,\Omega$ $N = 1023$, $K = 20$

APD Gain	Probability of Error, P_e			
	p = 50 pW	p = 100 pW	p = 500 pW	p = 1000 pW
1	.487E+00	.474E+00	.373E+00	.299E+00
5	.435E+00	.373E+00	.563E-01	.124E-02
10	.373E+00	.260E+00	.132E-02	.131E-06
15	.314E+00	.169E+00	.162E-04	.952E-16
20	.260E+00	.103E+00	.262E-06	.101E-11
25	.213E+00	.599E-01	.900E-08	.696E-13
30	.171E+00	.336E-01	.710E-09	.149E-13
35	.137E+00	.185E-01	.116E-09	.631E-14
40	.109E+00	.102E-01	.339E-10	.402E-14
45	.863E-01	.582E-02	.152E-10	.332E-14

Table 5.6
P_e Versus APD gain
R = 91KΩ N = 1023

| APD Gain | Probability of Error, P_e | | | |
| | P = 100 pW | | p = 500 pW | |
	K = 20	K = 50	K = 20	K = 50
1	.250E+00	.251E+00	.840E-03	.211E-02
5	.124E-02	.403E-02	.420E-13	.315E-06
10	.155E-05	.257E-03	.911E-15	.199E-06
15	.678E-07	.147E-03	.833E-15	.246E-06
20	.277E-07	.163E-03	.140E-14	.332E-06
25	.297E-07	.219E-03	.275E-14	.452E-06
30	.467E-07	.305E-03	.558E-14	.612E-06
35	.844E-07	.424E-03	.112E-13	.820E-06
40	.157E-06	.579E-03	.222E-13	.108E-05
45	291E-06	.773E-03	.431E-13	.142E-05

Table 5.7
P_e Versus APD gain
R = 500KΩ N = 1023

| APD Gain | Probability of Error, P_e | | | |
| | p = 100 pW | | p = 500 pW | |
	K = 20	K = 50	K = 20	K = 50
1	.603E-01	.661E-01	.280E-08	.416E-05
5	.120E-06	.842E-04	.190E-15	.117E-06
10	.114E-08	.435E-04	.197E-15	.155E-06
15	.114E-08	.652E-04	.428E-15	.221E-06
20	.271E-08	.107E-03	.982E-15	.313E-06
25	.736E-08	.171E-03	.221E-14	.436E-06
30	.192E-07	.262E-03	.482E-14	.598E-06
35	.467E-07	.384E-03	.101E-13	.807E-06
40	.104E-07	.541E-03	.206E-13	.107E-05
45	.217E-06	.736E-03	.407E-13	.140E-05

Table 5.8 : P_e Versus optical power

N = 511

Probability of Error, P_e

Optical power, watts	K = 10			K = 20		K = 50	
	R = 1KΩ	R = 9KΩ	R=500KΩ	R = 1KΩ	R = 500KΩ	R = 1KΩ	R=500KΩ
.1E-10	.147E+00	.182E-01	.490E-02	.208E+00	.265E-01	.277E+00	.911E-01
.5E-10	.197E-02	.331E-06	.755E-08	.138E-01	.218E-04	.592E-01	.358E-02
.1E-09	.116E-04	.621E-10	.138E-11	.733E-03	.353E-06	.138E-01	.700E-03
.2E-09	.372E-08	.151E-13	.996E-15	.108E-04	.132E-07	.219E-02	.206E-03
.5E-09	.256E-13	.117E-16	.357E-17	.416E-07	.110E-08	.269E-03	.847E-04
.7E-09	.797E-15	.258E-17	.113E-17	.925E-08	.671E-09	.161E-03	.709E-04
.1E-08	.454E-16	.835E-18	.485E-18	.277E-08	.463E-09	.107E-03	.622E-04
.1E-07	.120E-18	.955E-19	.927E-19	.247E-09	.223E-09	.493E-04	.479E-04
.1E-06	.824E-19	.815E-19	.814E-19	.212E-09	.211E-09	.469E-04	.468E-04

Table 5.9 : P_e Versus optical power

N = 1023

Probability of Error, P_e

	K = 20				K = 40				K = 80		
R=1KΩ	R=9KΩ	R=91KΩ	R=500KΩ	R=1KΩ	R=9KΩ	R=91KΩ	R=500KΩ	R=1KΩ	R=9KΩ	R=91KΩ	R=500KΩ
.11E-01	.80E-03	.30E-04	.19E-05	.38E-01	.78E-02	.13E-02	.32E-03	.85E-01	.33E-01	.12E-01	.61E-
.32E-03	.31E-05	.26E-07	.93E-09	.43E-03	.34E-03	.30E-04	.64E-05	.22E-02	.56E-02	.16E-02	.80E-
.61E-06	.10E-08	.61E-11	.32E-12	.12E-03	.52E-05	.49E-06	.13E-06	.30E-02	.62E-03	.21E-03	.11E-
.65E-11	.21E-13	.76E-15	.15E-15	.39E-06	.31E-07	.77E-08	.40E-08	.16E-03	.52E-04	.28E-04	.21E-
.11E-12	.10E-14	.84E-16	.26E-16	.61E-07	.82E-08	.29E-08	.18E-08	.68E-04	.28E-04	.18E-04	.14E-
.32E-14	.89E-16	.15E-16	.68E-17	.12E-07	.28E-08	.13E-08	.99E-09	.32E-04	.17E-04	.12E-04	.11E-
.61E-18	.47E-18	.42E-18	.40E-18	.32E-09	.29E-09	.28E-09	.28E-09	.64E-05	.62E-05	.61E-05	.60E-

Table 5.10
P_c Versus no. of users

N = 511   R = 500K Ω

K	Probability of Error, P_e			
	p = 100 pW	p = 200 pW	p = 1000 pW	p=10000 pW
10	.138E-11	.996E-15	.485E-18	.927E-19
20	.353E-06	.132E-07	.463E-09	.223E-09
30	.209E-04	.257E-05	.320E-06	.203E-06
40	.185E-03	.397E-04	.867E-05	.623E-05
50	.700E-03	.206E-03	.622E-04	.479E-04

Table 5.11

P_e Versus no. of users

N = 1023   R = 500K Ω

K	Probability of Error, P_e		
	p=500 pW	p = 1000 pW	p = 10,000 pW
20	.155E-15	.686E-17	.409E-18
30	.126E-10	.183E-11	.322E-12
40	.405E-08	.99 E-09	.280E-09
50	.120E-06	.396E-07	.145E-07
60	.118E-05	.480E-06	.213E-06
70	.625E-05	.291E-05	.145E-05
80	.216E-04	.111E-04	.609E-05
90	.563E-04	.313E-04	.184E-04
100	.124E-03	.735E-04	.456E-04

Table 5.12 : P_e versus bias resistance

N = 511   K = 25

R (ohms)	Probability of Error, P_e							
	$\langle g \rangle = \langle g \rangle_{opt}$				$\langle g \rangle = 1$			
	p=100pW	p=1000 pW	p= .01μW	p= .1 μW	p = 100 pW	p=1000 pW	p= .1 μW	p = .1μW
10	.15E+00	.13E-03	.32E-07	.13E-07	.49E+00	.49E+00	.43E+00	.75E-01
100	.25E-01	.78E-06	.16E-06	.12E-07	.49E+00	.44E+00	.10E+00	.81E-04
1000	.17E-02	.86E-07	.14E-07	.12E-07	.47E+00	.26E+00	.38E-03	.41E-04
10000	.12E-03	.38E-07	.13E-07	.12E-07	.41E+00	.26E-01	.52E-04	.40E-04
100000	.13E-04	.26E-07	.13E-07	.12E-07	.24E+00	.29E-03	.41E-04	.40E-04
500000	.39E-05	.22E-07	.13E-07	.12E-07	.71E-01	.69E-04	.40E-04	.40E-04
1000000	.25E-05	.21E-07	.13E-07	.12E-07	.26E-01	.55E-04	.40E-04	.40E-04

Table 5.13

P_e Versus Bias Resistance

K = 1023   K = 50

| R, Ω	Probability of Error, P_e			
	p=100 pW	p=1000 pW	p = 100 pW	p= 1000 pW
10	0.499E+00	0.493E+00	0.208E-00	0.590E-07
100	0.494E+00	0.448E+00	0.585E-01	0.208E-07
1000	0.474E+00	0.260E+00	0.809E-02	0.163E-07
10000	0.412E+00	0.198E-01	0.992E-03	0.152E-07
100000	0.241E+00	0.742E-05	0.135E-03	0.147E-07
500000	0.661E-01	0.114E-06	0.426E-04	0.145E-07
1000000	0.210E-01	0.522E-07	0.278E-04	0.145E-07
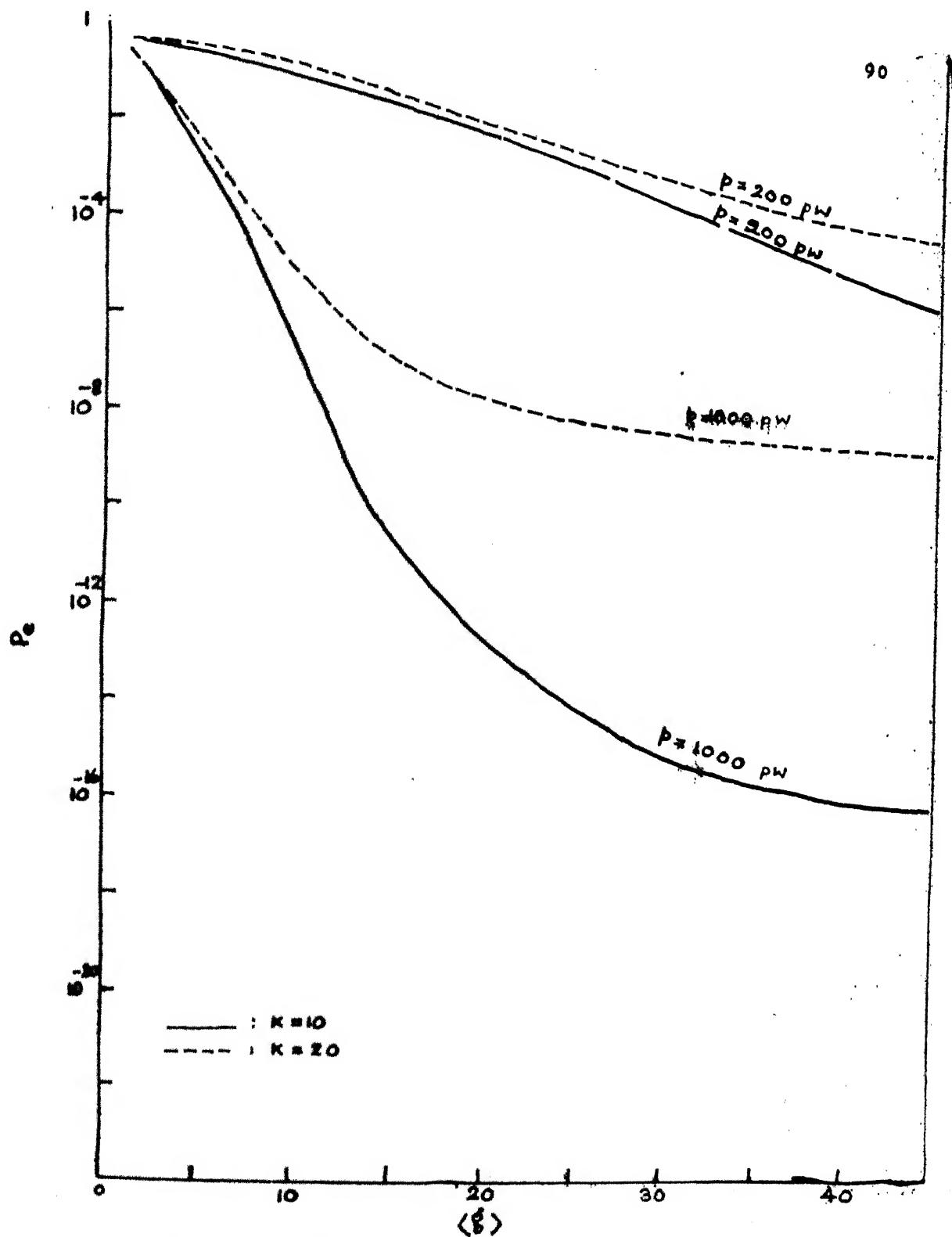
FIG. 5.1. P_e VARIATION WITH APD GAIN FOR R=1K, N=511
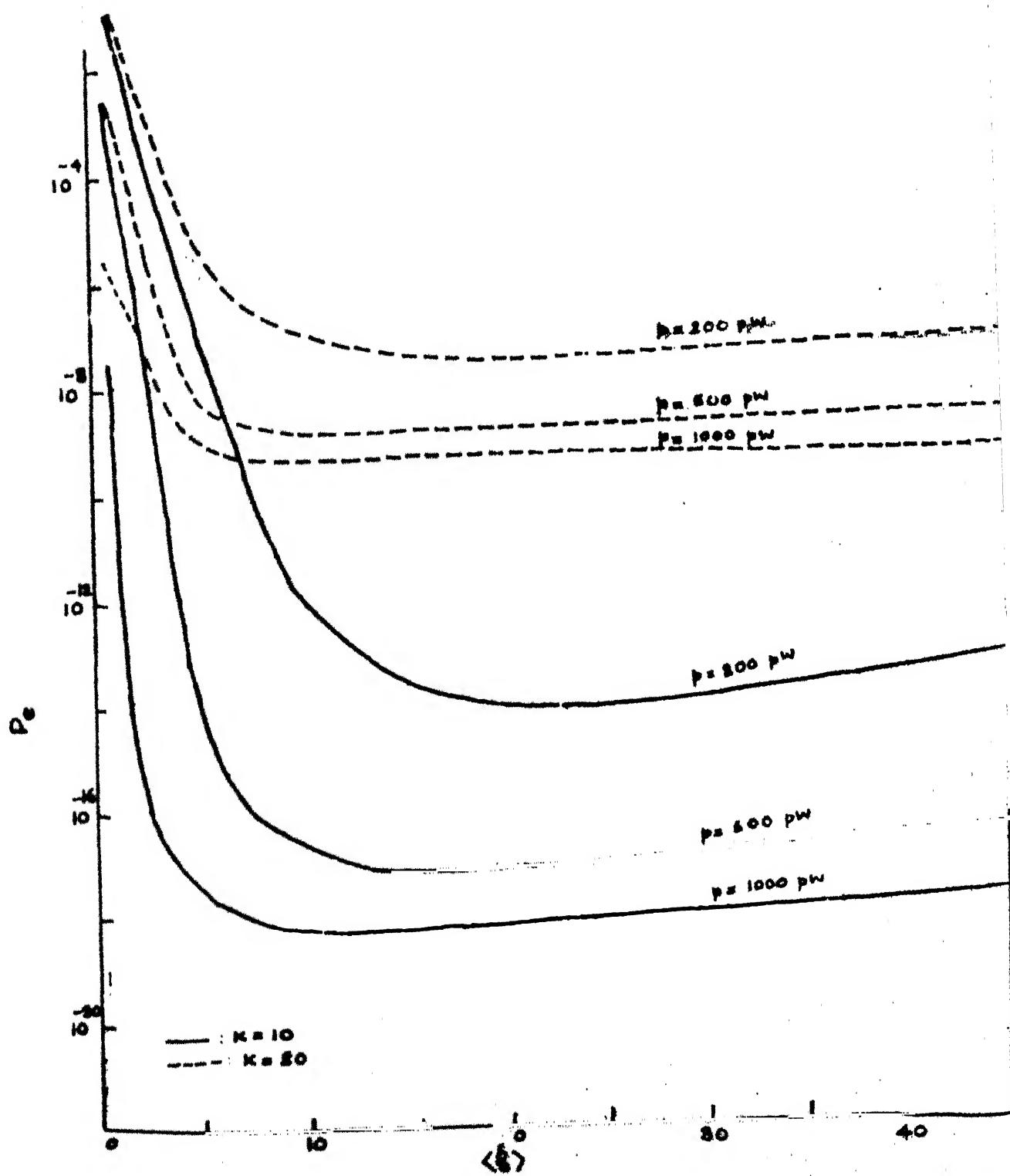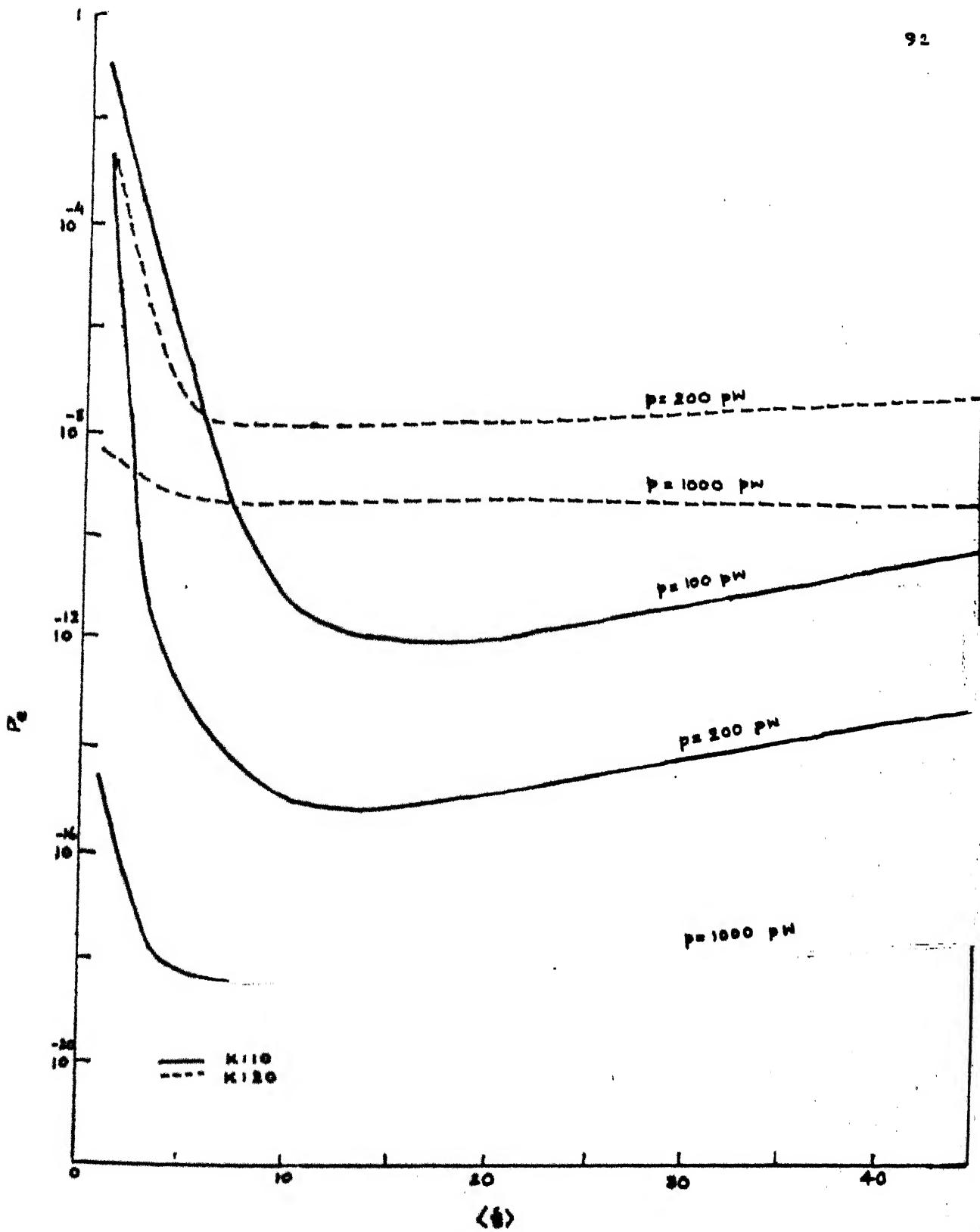
FIG 8.2 P_e variation with APD gain for R=500K, N=811
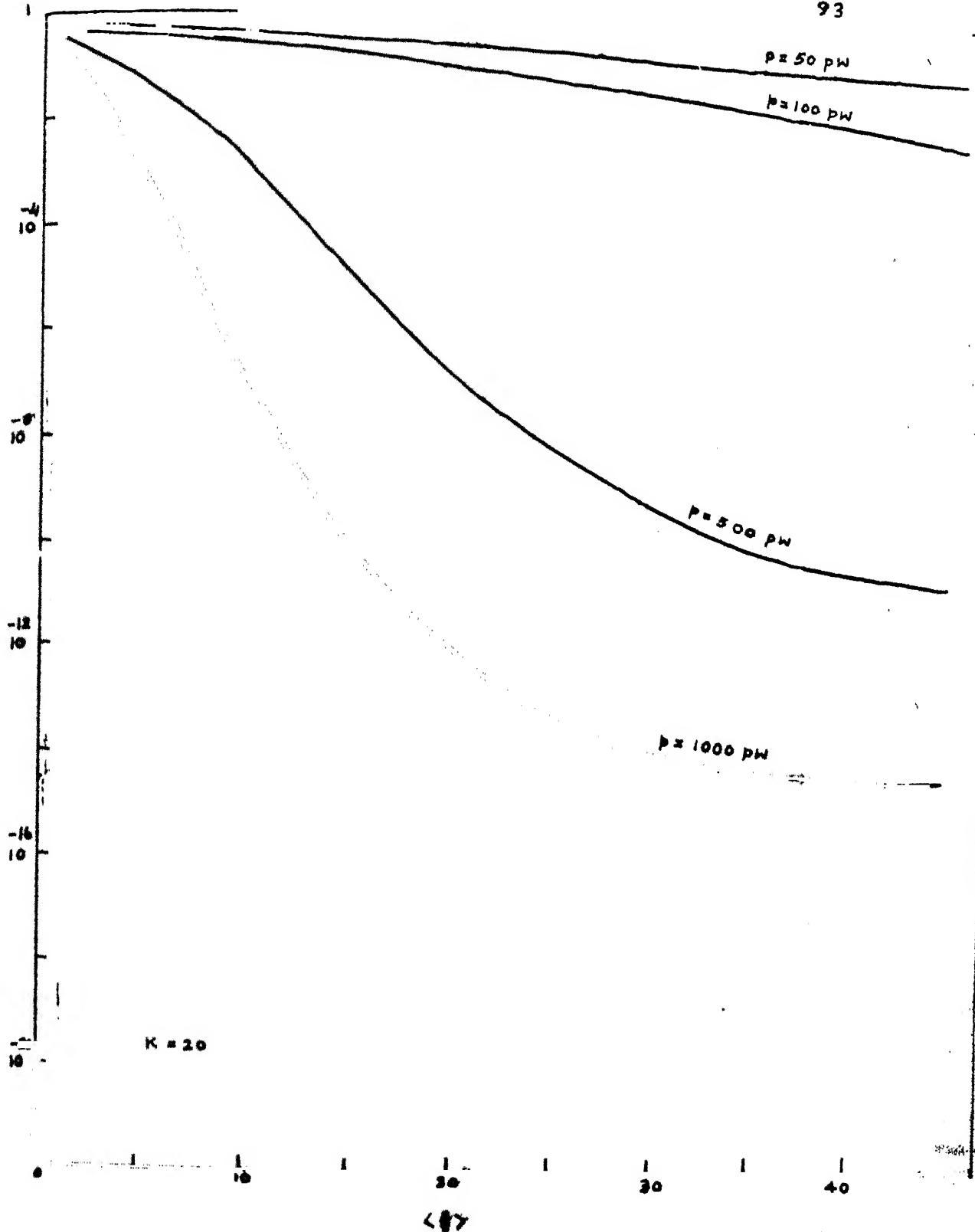
FIG. 8.4 P_e VARIATION WITH APD GAIN FOR R=1K, N=1022
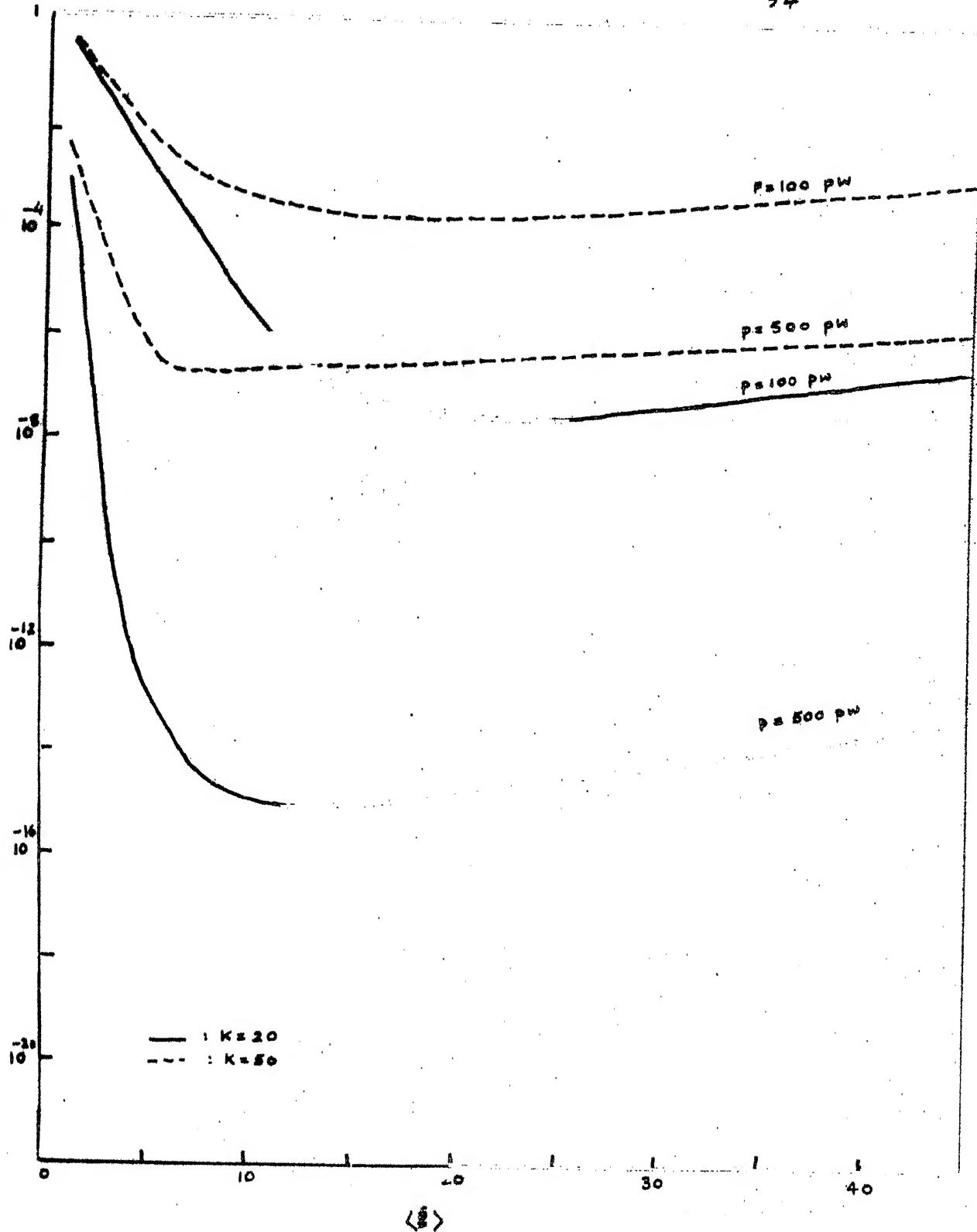
FIG.5.5. P_B VARIATION WITH APD. GAIN FOR $R=91K$, $N=1023$
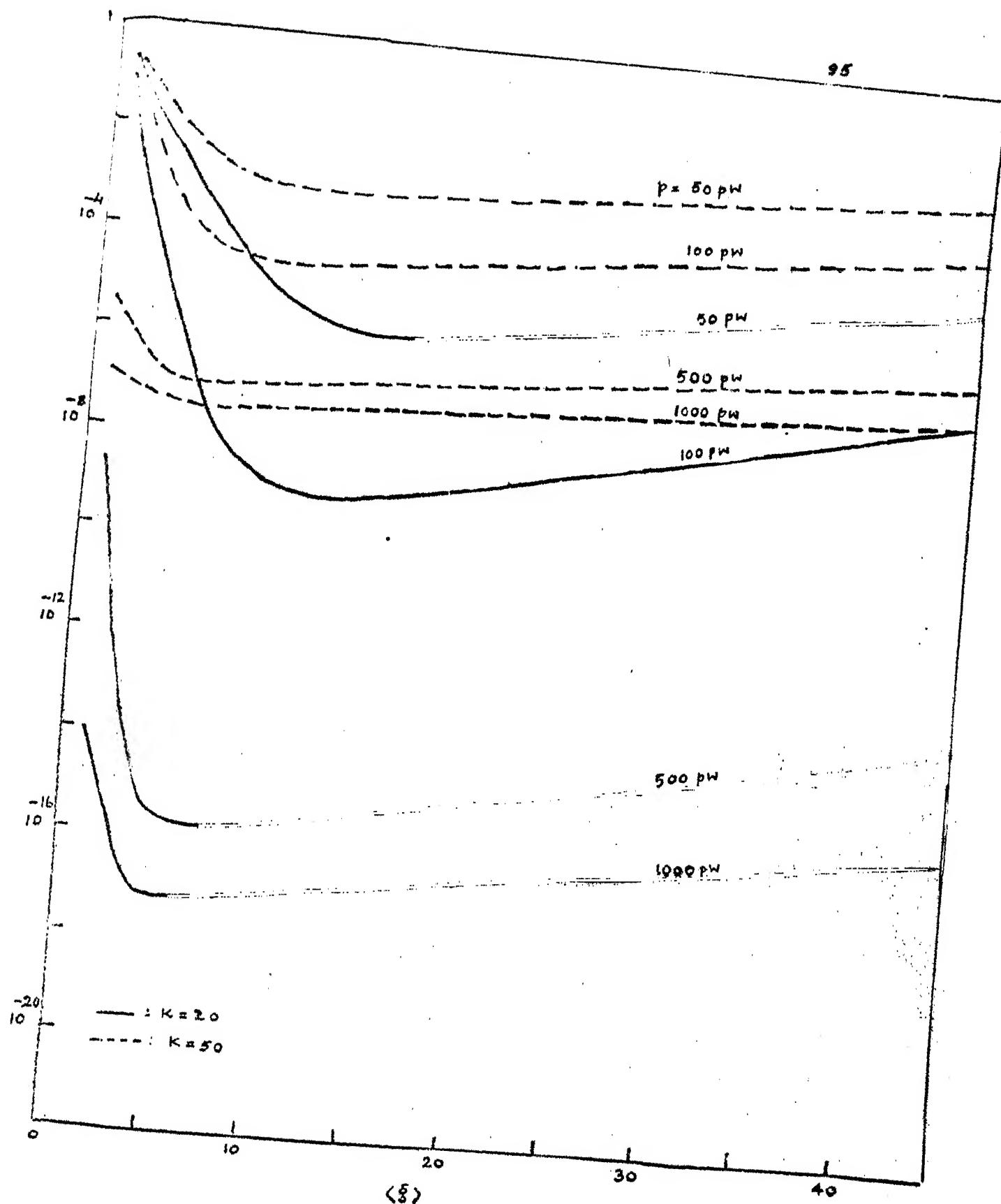
FIG 5.6 P_e VARIATION WITH APD GAIN FOR $R = 500K$, $N = 1023$
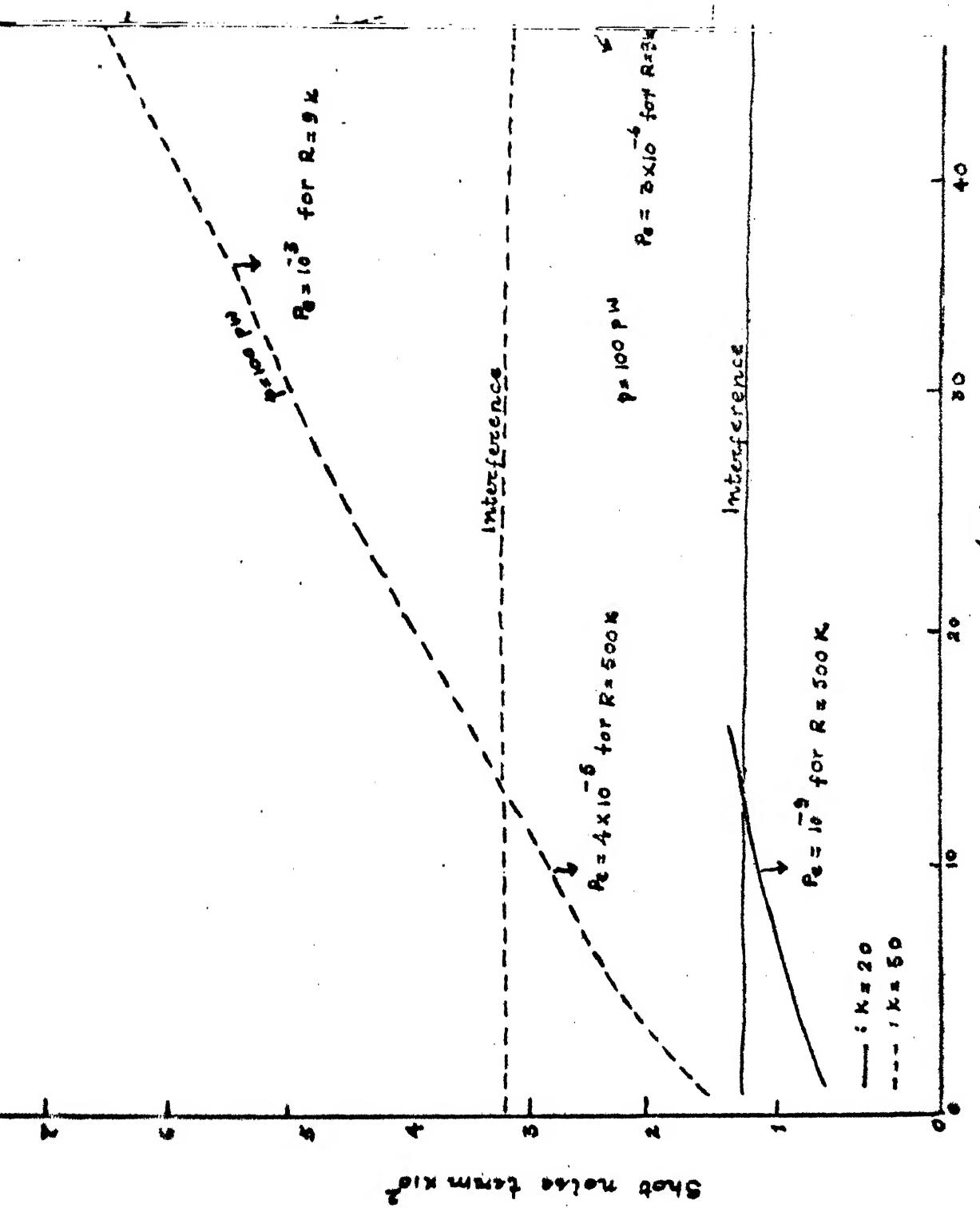
Fig. 6.6 : Shot Noise Variation with APD gain.

Shot noise term $\times 10^2$

1.7×10^{-4} at $R=3k$

$R_e = 7 \times 10^{-9}$ for $R=50k$

interference

(S)
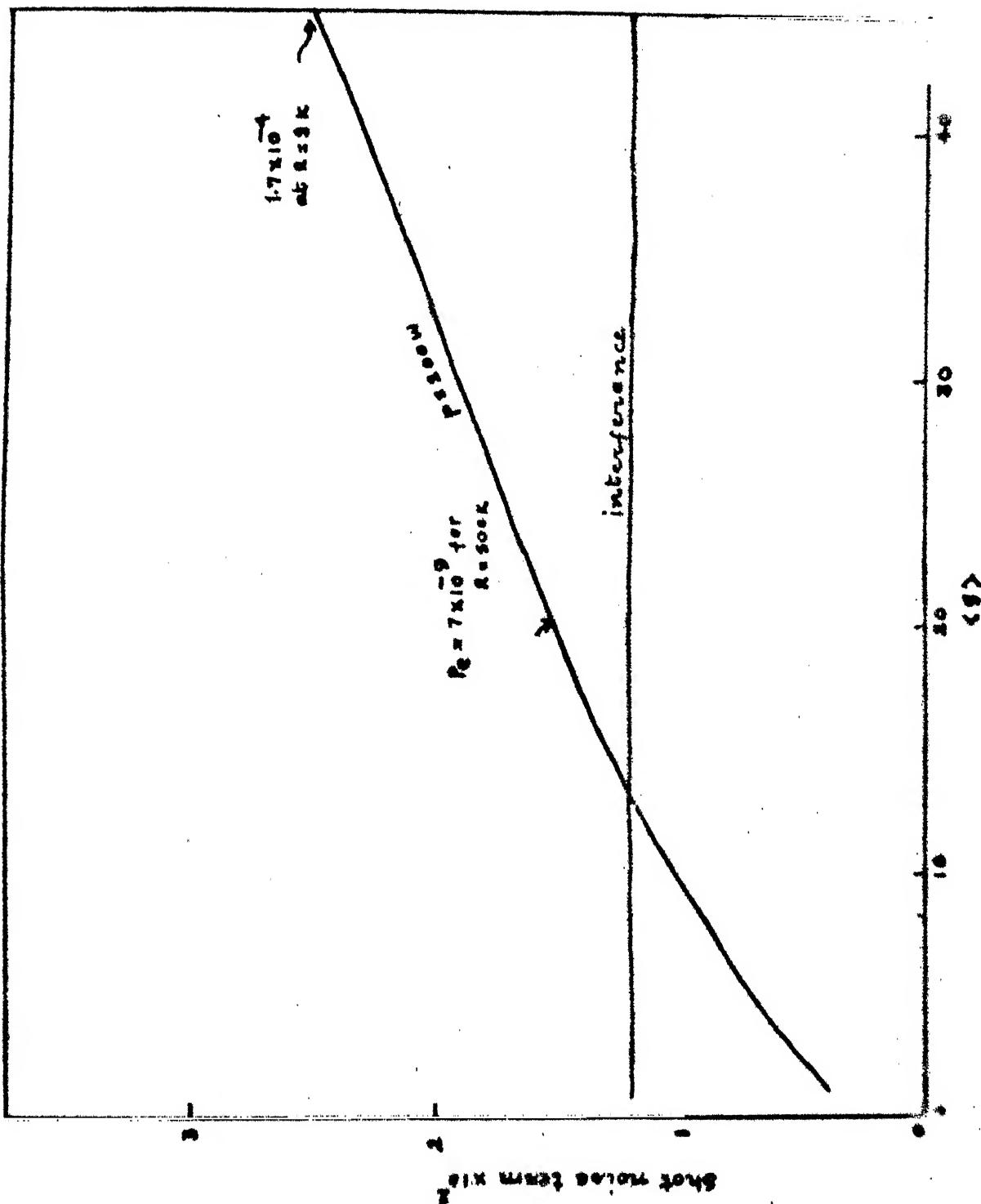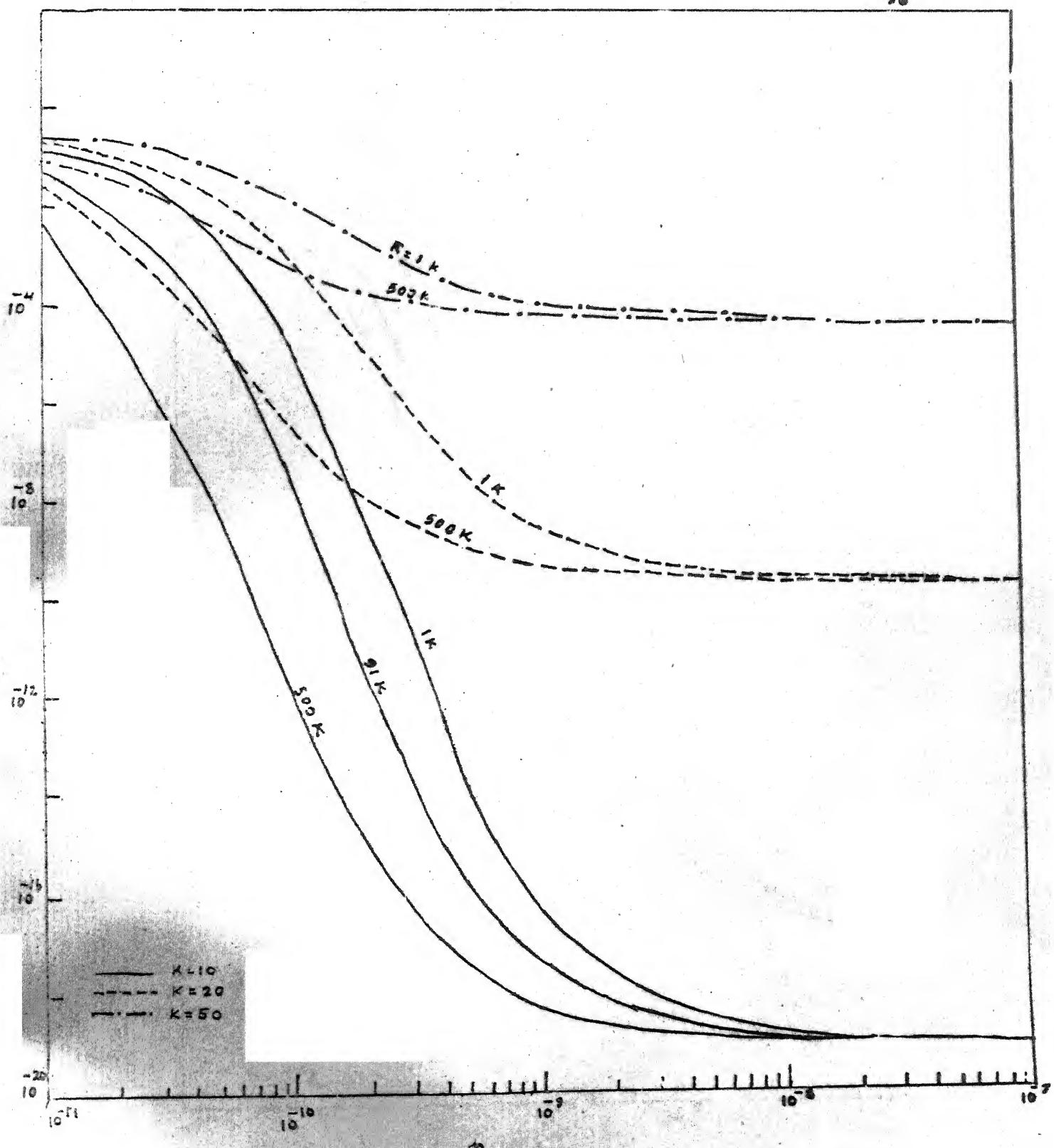
FIG 5.7. P_e VARIATION WITH OPTICAL POWER p IN WATTS . FOR $N=511$
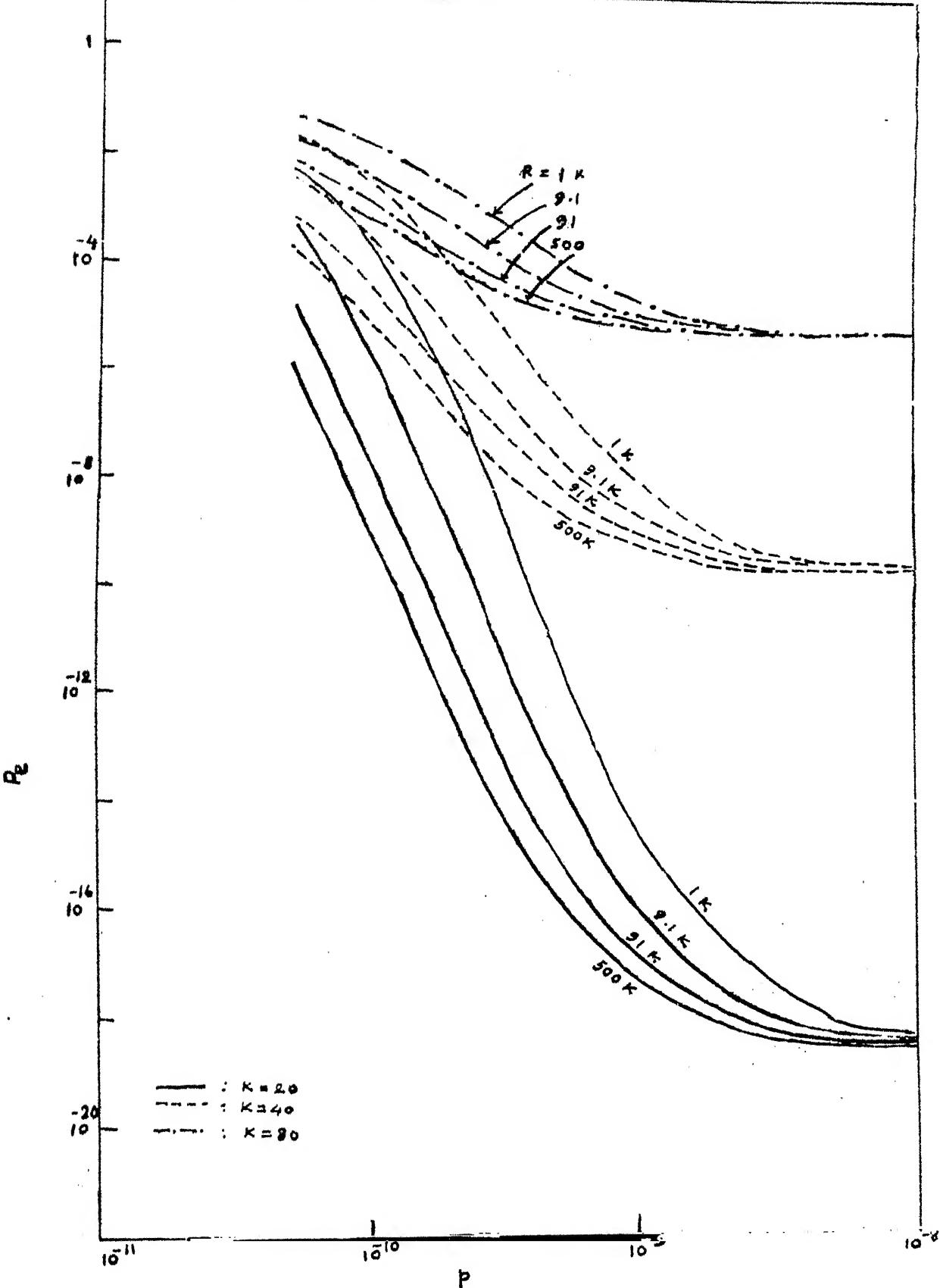
FIG 5·8. P_e VARIATION WITH OPTICAL POWER p IN WATTS

F·R N=1023
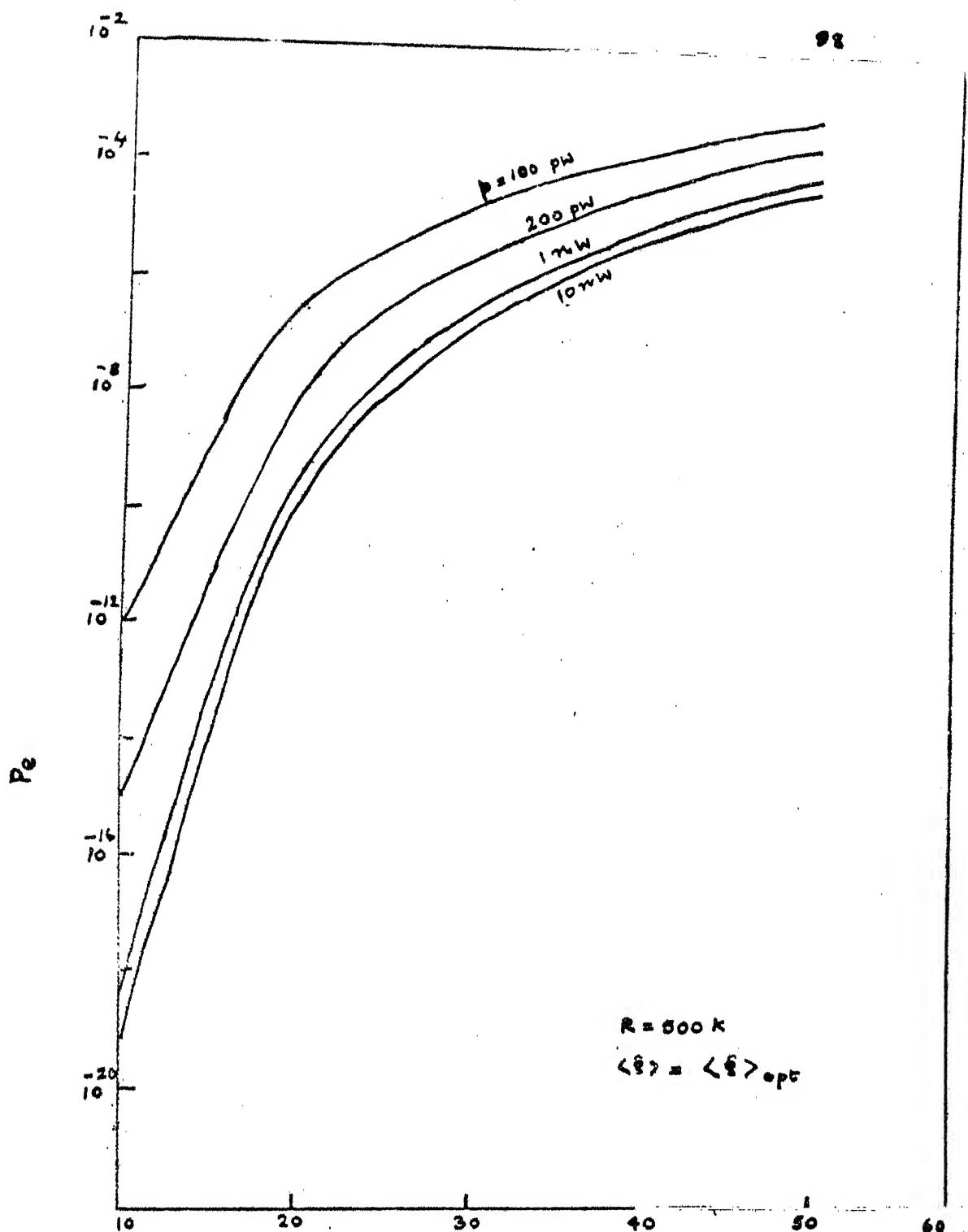
FIG 5.9 P_e VARIATION WITH NR. OF USERS K FOR N=511
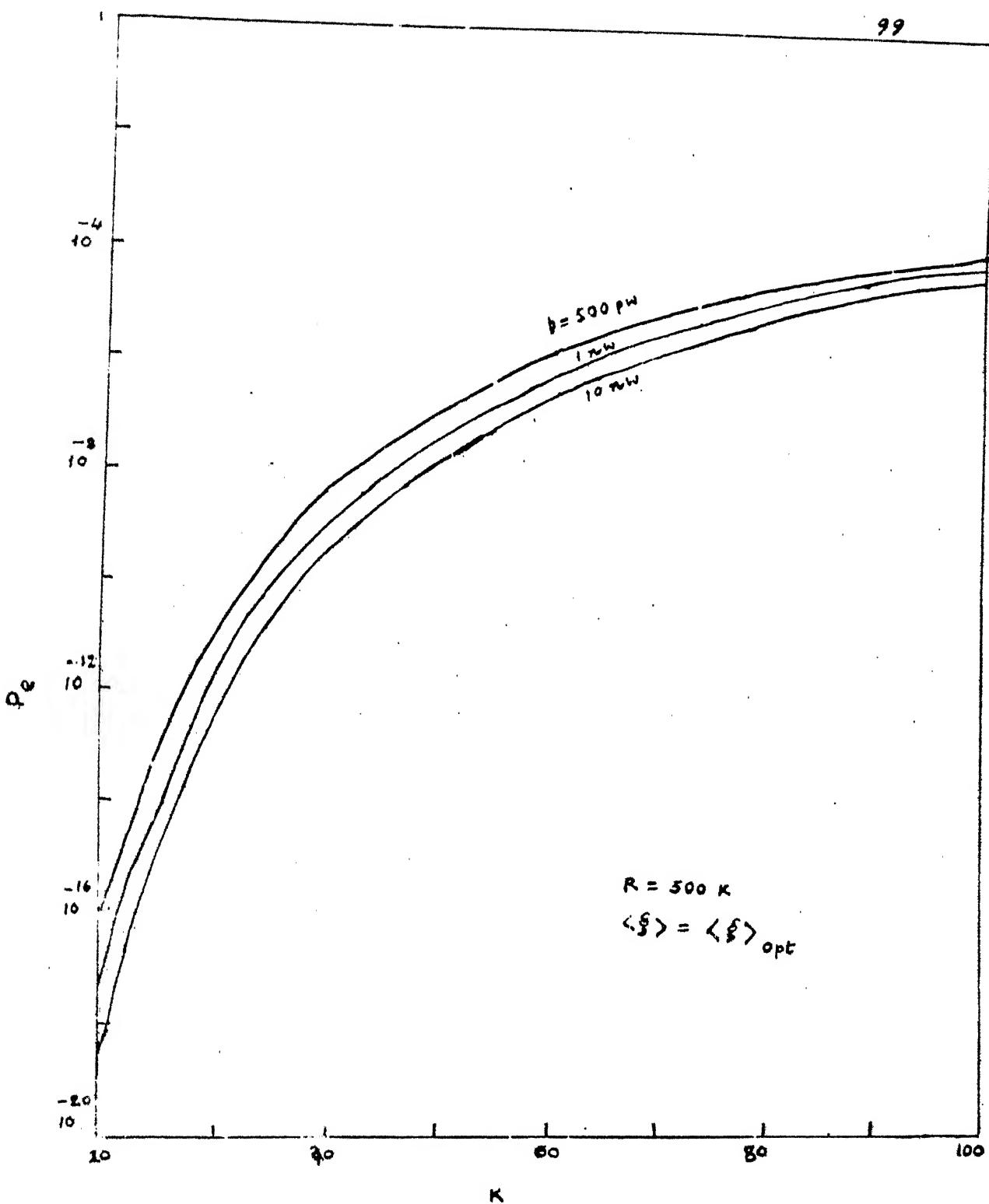
FIG 5.10 P_e VARIATION WITH NR. OF USERS FOR $N = 1023$
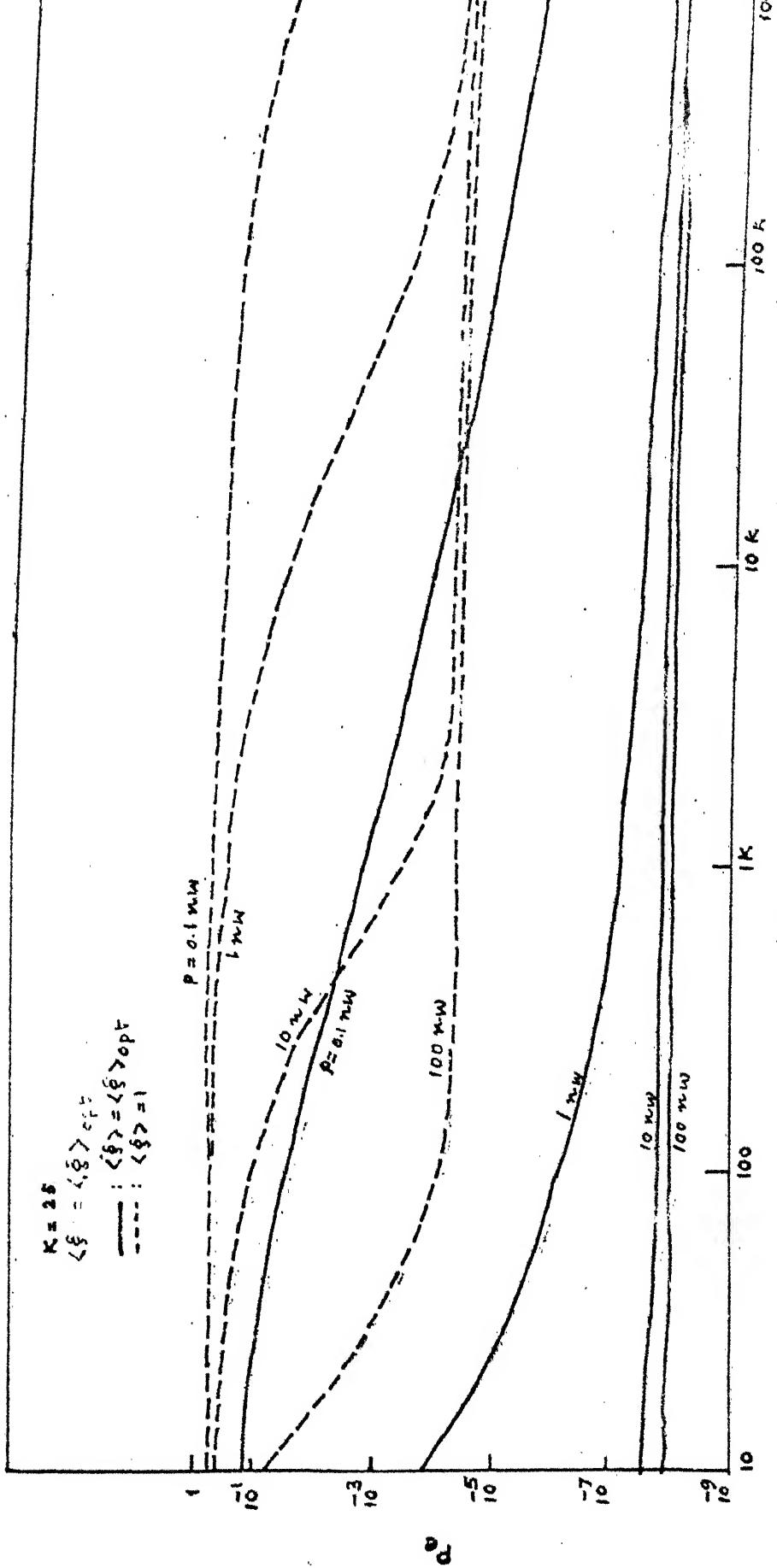
FIG 5.11: P VARIATION WITH BIAS RESISTANCE, R IN OHMS, FOR M=5[?]
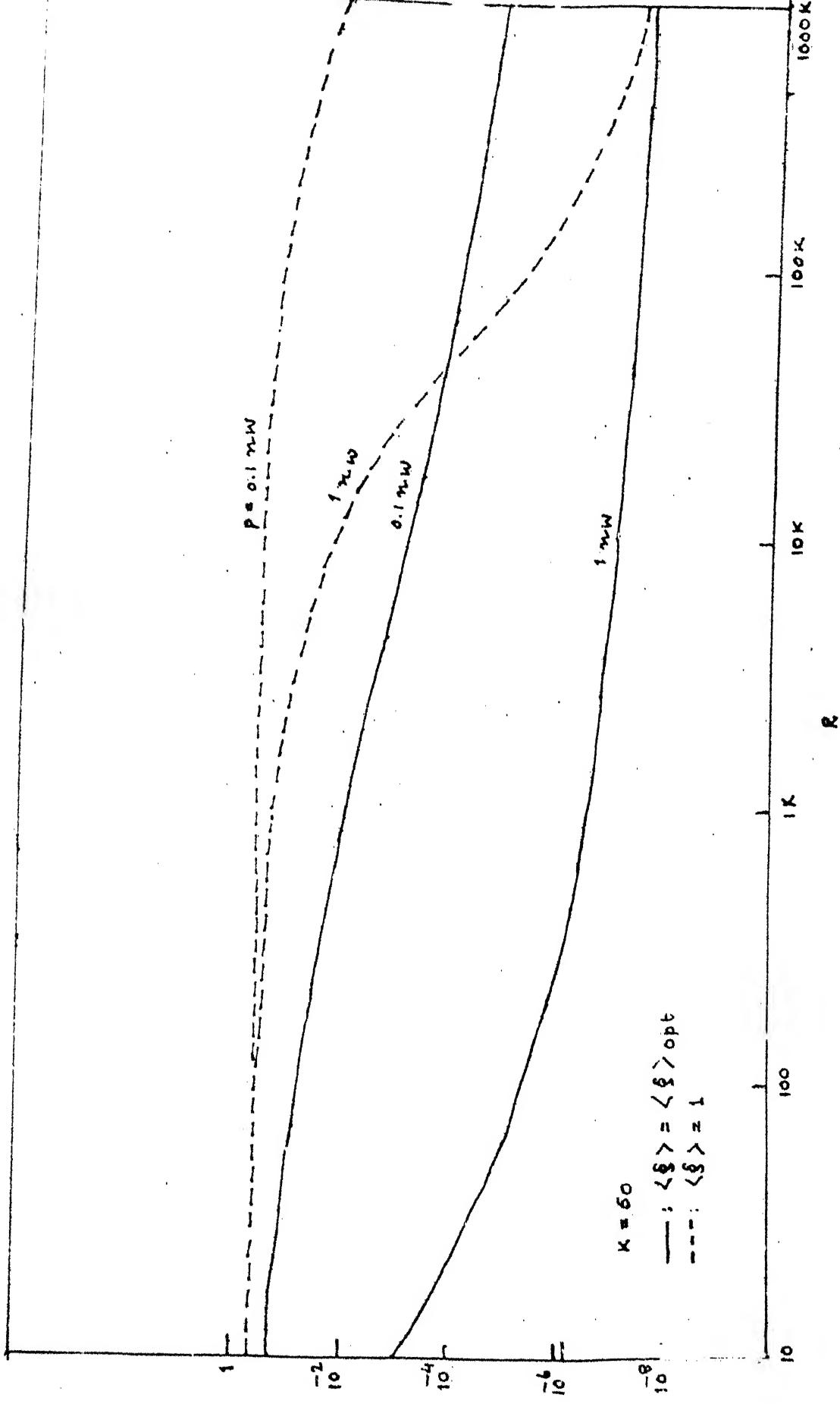
FIG. 5.12 P_e VARIATION WITH BIAS RESISTNCE R IN OHMS FOR N = 1023

APPENDIX A

SELECTION AND GENERATION OF GOLD SEQUENCES

As we have seen in Chapter 3, Gold sequences are large in number for a given code sequence length, N and also possess low cross correlation properties. For a given N, they can be selected as follows.

Let $f_1(x)$ be the minimal polynomial of the primitive element $\alpha \in GF(2^n)$ and $f_t(x)$ be the minimal polynomial of α^t where $f_1(x)$ and $f_t(x)$ are of degree n and if n and t are such that

$$t = 2^{n+1/2} + 1, \qquad n \quad odd$$

$$= 2^{n+2/2} + 1, \qquad n \quad even$$

then the product $f(x) \triangleq f_1(x)f_t(x)$ determines a linear feedback shift register (LFSR) which generates the 2^n+1 different Gold sequences (corresponding to the 2^n+1 states in distinct cycles) of period (or length) $N = 2^n-1$[1]. To state this in terms of the M-sequences generated by LFSRs corresponding to $f_1(x)$ and $f_1(x)$ let u be the M-sequence generated by an LFSR corresponding to $f_1(x)$ and v be the similar M-sequence corresponding to $f_t(x)$. Then the set of Gold sequences G(u,v) is given by [22]

$$G(u,v) = \{u, v, \ u \oplus v, \ u \oplus Tv, \ u \oplus T^2y, u \oplus T^3v, \ldots u \oplus T^{N-1}v\}$$

where $\oplus$ indicates term wise modulo-2 addition of the two sequences and $T^i\omega$ indicates the ith cyclic shift of the sequence ω. It is to be noted that in the above set, except for u and v any other sequence is not an M-sequence, i.e. they do not have the properties of M-sequences. The generation of Gold sequences is clear from the above. This can be generated in 2 ways. One is to have an LFSR corresponding to $f(x)$ and generate the different sequences by inserting different initial states into the LFSR. The other method is to have two LFSR's corresponding to $f_1(x)$ and $f_t(x)$ and take the modulo 2 sum of their outputs. We have indicated both the methods in Fig. A.1 for

$$f_1(x) = 1+x^2+x^5 \text{ and } f_t(x) = f_9(x) = 1+x^2+x^4+x^5,$$

since $t = 2^{5+1/2}+1 = 9$

The polynomials are commonly represented. in octal notation. Then $f_1(x)$ is represented as 25(=100101) and $f_t(x)$ as 65(=110101).

In our case we choose [26] the polynomials for n=9,10 corresponding to N=511 and 1023 respectively as given below in octal notation.

| N	n	t	$f_1(x)$	$f_t(x)$
511	9	33	1021	1333
1023	10	65	2011	3515
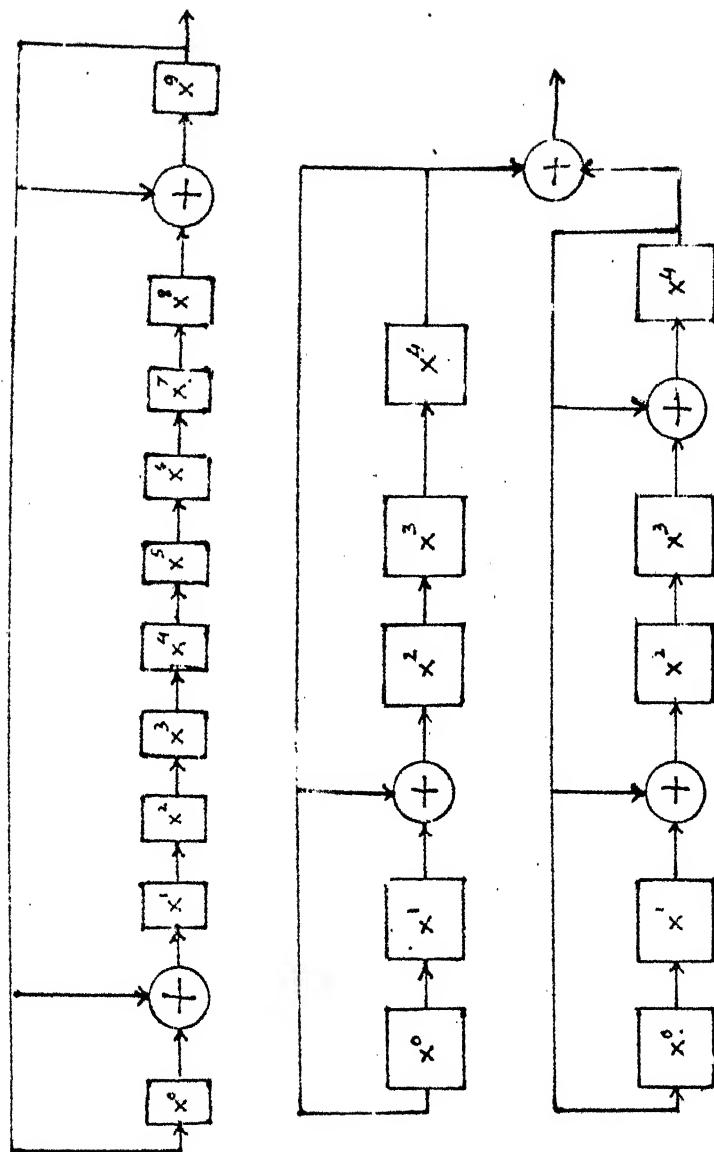
FIG. A.1.: GENERATION OF GOLD SEQUENCES
USING: (a) $f(x)$ (b) $f_1(x)$ and $f_t(x)$

APPENDIX B

COMPUTER SIMULATION

As stated in Chapter 4, we made simulations for the unlimited bandwidth receiver. The simulations are made for only unit APD gain because of the difficulty in generating the random gains with its probability density functions which is quite complex. We know the intensity $\lambda(t)$ is given by

$$\lambda(t) = \frac{\eta b_E}{h\gamma T} \left(K + \sum_{i=1}^{K} d_i(t - \tau_i) a_i(t - \tau_i) \right) \qquad (B.1)$$

The term inside the brackets changes between O and $2K$. Also it changes, say for $t \in (O, T)$, possibly for each of the chip intervals. So to simplify the situation we assumed τ_i to be taking only discrete values which are multiples of T_c, the chip duration. This makes $\lambda(t)$ to have a fixed value during each chip interval, through randoms because of the randomness of d_i, $2 \leq i \leq K$. We removed the $i=1$ case because we assume the data bits of user 1 signal to be all ones. Such an assumption does not lead to any inferior performance. The simulation is performed as follows:

1. The random delays τ_i's are generated using uniform distribution for integers between zero and N.

2. The data bits $d_{i,-1}$, $d_{i,o}$ are generated for each i assuming the correlation interval to be in (o, T). The PN-sequences

$a_i(t)$, $2 \leq i \leq K$ are modified by these τ_i's and d_i's and added to $a_1(t)$ to get the $\lambda(t)$ for $t \in (o,T)$.

3. Using this $\lambda(t)$ we generate N Poisson random variables corresponding to each chip interval. These Poisson random variables represent the total number of electrons emitted in that chip interval. The emission time instants are not important to us because the correlating PN sequence has constant value (or it integrates over the chip interval) in each chip interval. So these Poisson random variables are weighted by the corresponding N chip values of $a_1(t)$ and summed up to get the shot noise signal contribution to the decision statistic.

4. We then generate a Gaussian random variable and add this to the above quantity to make the total decision statistic. We compare this statistic to the threshold and decide as the data bits of user 1 signal.

Since detection of each data bit needs the generation of N Poisson random variables, the computation time required is very high. For a data length of 1000 bits the computation time required is about one hour for N=511. So higher values of N are not considered.

The program listing of the simulation is given after the list of References.

REFERENCES

1. R.L. Pickholtz, D.L. Schilling, and L.B. Milstein, 'Theory of Spread Spectrum Communications - A Tutorial', IEEE Transactions on Communications, COM-30, No.5, pp 855-884, May 1982.

2. T.Li, 'Optical Fiber Communication - The State of the Art', IEEE Transactions on Communications, COM-26, No. 7, pp 946-955, July 1978.

3. B. HiroSaki, S. Hasegawa, and A. Sawai, 'Spread Spectrum Multiple Access Data Loop', Conference Record of National Telecommunication Conference, 1981, paper G 8.5.

4. E.L. RawSon and R.M. Met ^{C}alfe, 'Fibernet: Multimode Optical Fibers for Local Computer Network', IEEE Transactions on Communications, COM-26, pp 983-990, June, 1978.

5. S.D. Personick, 'Baseband Linearity and Equalization in Fibre Optic Digital Communication System', BSTJ, Vol. 52, No. 7, pp 1175-1194, September 1973.

6. R.M. Gagliardi and S. Karp, 'Optical Communications', John Wiley and Sons, New York, 1976.

7. I. Bar-David,''Communication under the Poisson Regime', IEEE Transactions on Information Theory, IT-15, No. 1, pp 31-37, January 1969.

8. G.J. Foschini, R.D. Gitlin, and J. Salz, 'Optimum Direct Detection for Digital Fibre Optic Communication Systems', BSTJ, Vol. 54, No. 8, pp 1389-1430, October 1975.

9. G.D. Forney, ' Maximum - Likelihood Sequence Estimation of Digital Sequence in the Presence of Inter Symbol Interference', IEEE Transactions on Information Theory, IT-18, No. 3, pp 363-378, May 1972.

10. Govind Sharma, 'A Quantized Electron Arrival Times Estimator Based Digital Fibre Optic Receiver', M.Tech Thesis, I.I.T. Kanpur, August 1981.

11. R.Dogliotti, A.Guardincerri, and A. Lurison, 'Baseband equalization in fiber optic digital transmission', Optical and Quantum Electronics, Vol. 8, pp 343-353, 1976.

12. D.G. Messerschmitt, 'Minimum MSE Equalization of Digital Fibre Optic Systems', IEEE Transactions on Communications, COM-26, No..7, pp 1110-1118, July 1978.

13. S.D. Personick, 'Receiver Design for Digital Fibre Optic Communication Systems', Part I and Part II, BSTJ, Vol. 52, No. 6, pp 843-886, July-August 1973.

14. C.A. Laber, M. Kaveh, 'Spread Spectrum Signalling for distributed Fiber Optic Systems', IEEE, Transactions on Aerospace and Electronic Systems, AES-16, No. 4, pp 440-445, July 1980.

15. S.D. Personick, P. Balaban, J.H. Bobsin, and P.R. Kumar, 'A detailed Comparison of Four Approaches to the Calculation of the sensitivity of optical fiber system receivers', IEEE Transactions on Communications, COM-25, pp 541-548,May 1977.

16. M.B. Pursley., 'Performance evaluation for phase-coded Spread Spectrum Multiple-Access Communication - Part I: System Analysis', IEEE Transactions on Communications, COM-25, pp 795-799, August 1977.

17. M.B. Pursley and D.V. Sarwate, 'Performance evaluation for phase coded Spread Spectrum Multiple Access - Part II: Code Sequence Analysis', IEEE Transactions on Communications, COM-25, pp 800-803, August 1977.

18. H.L. Van Trees, 'Detection, Estimation, and Modulation Thoery', Vol. 1, John Wiley and Sons, New York, 1969.

19. M.B. Pursley, 'Spread-Spectrum Multiple Access Communications in Multi-user Communication Systems, G. Longo, Ed. Springer-Verlag, New York, pp 139-199, 1981.

20. M.B. Pursley and D.V. Sarwate, 'Evaluation of correlation parameters for periodic sequences', IEEE Transactions on Information Theory, IT-23, pp 508-513, July, 1977.

21. K. Yao, 'Error probability of asynchronous Spread Spectrum Multiple-Access Communication Systems', IEEE Transactions on Communications, COM-25, pp 803-809, August 1977.

22. D.V. Sarwate and M.B. Pursley, 'Cross correlation properties of pseudo-random and related sequences', Proceedings IEEE, Vol. 68, pp 593-619, May 1980.

23. M. Mansuripur, J.W. Goodman, E.G. Rawson, and R.E. Norton, 'Fibre optic receiver error rate prediction using the Gram-Charlier series', IEEE Transactions on Communications, COM-28, No. 3, pp 402-407, March 1980.

24. J.K. Skwirzynski,ed., 'New Concepts in Multi-user Communication', Sijthoff and Noordhoff International, The Netherlands, 1981.

25. A. Papoulis, 'Probability, Random variables,and Stochastic processes', McGraw Hill, Tokyo, 1972.

26. R.C. Dixon, 'Spread Spectrum Systems', John Wiley and Sons, New York, 1976.

27. R.C. Dixon, ed., 'Spread Spectrum Techniques', IEEE Press, New York, 1976.

28. G.K. Huth, 'Optimization of Coded Spread Spectrum Systems performance', IEEE Transactions on Communications, COM-25, pp 763-770, Aug 1977.

29. M.E. Austin, 'Decision-Feedback Equalization for Digital Communication over dispersive channels', MIT RLE Technical Report 461, August 11,1967.

```
*********************************************************
PROGRAM TO SIMULATE THE FIBER OPTIC SSMA SYSTEM FOR
THE UNLIMITED BANDWIDTH CASE
*********************************************************
      INTEGER TD(25),A(25,0:511),B(0:511),POISS(0:511)
      DIMENSION R(10000),MB(25,0:511)
      COMMON MB,A,B
      INTEGER LAMDA(0:511),G05DYF,G05EYF
      REAL LSHOT,LGAUSS,LTOT
      LOGICAL D(25,0:1),DB(1000),INTR,G05DZF
      OPEN(UNIT=18,DEVICE='DSK')
      OPEN(UNIT=30,DEVICE='DSK')
      OPEN(UNIT=31,DEVICE='DSK')
      N=511
      READ(30,*)ETAHNU,E,BZC,THETA,T,PWR,RES,K,DB
      CONST1=ETAHNU*PWR*T/N
      CONST3=SQRT(2.0*BZC*THETA*RES*T/(E*E))
      DO 10 I=1,K
      READ(18,5)(A(I,J),J=0,N-1)
      FORMAT(1X,160I2)
      CONTINUE
      IAVR=0
      DO 11 I=0,N-1
      IAVR=IAVR+A(1,I)
      CONTINUE
      IC=IAVR
      CONST2=ETAHNU*PWR*IC*K/N

   GENERATION OF RANDOM DELAYS TAU(I),2<I<K
   ---------------------------------------------

      DO 20 I=2,K
      TD(I)=G05DYF(1,N-1)
      CONTINUE
```

```
------------------------------------
SIMULATION STARTS HERE
------------------------------------

DO 40 J=1,LD

GENERATION OF BINARY R.V.FOR OTHER USER
DATA BITS D(1,-1),D(1,0)
------------------------------------------------

      IF(J.EQ.1)GOTO 14
      DO 13 I=2,K
      D(I,0)=G05DZF(0.5)
13    CONTINUE
      GOTO 16
14    DO 15 I=2,K
      D(I,0)=G05DZF(0.5)
      D(I,1)=G05DZF(0.5)
15    CONTINUE

MODIFICATION OF SEQS. ACC.TO D(1)'s AND TAU(1)'s
------------------------------------------------

16    CALL MODSEQ(K,TD,D,N)

CALCULATION OF LAMDA(t) _GENERATION OF POISSON R.V.
------------------------------------------------

      IFIL=0
      DO 25 I=0,N-1
      LAMDA(I)=(K+A(1,I)+B(I))
      CAPLMD=LAMDA(I)*CONST1
      NR=IFIX(20.0+20.0*SQRT(CAPLMD))
      CALL G05ECF(CAPLMD,R,NR,IFIL)
      POISS(I)=G05EYF(R,NR)
25    CONTINUE
```

OUTPUT OF CORRELATOR DUE TO SHOT NOISE

```
        SUM=0.0
        DO 30 I=0,N-1
        SUM=SUM+A(1,I)*POISS(I)
30      CONTINUE
        LSHOT=SUM*RES-CONST2
```

GENERATION OF GAUSSIAN RANDOM VARIABLE

```
        AWGN=GUSDDF(0.0,1.0)
        LGAUSS=AWGV*CONST3
        LTOT=LSHOT+LGAUSS
        IF(LTOT.GE.0.0)DB(J)=.TRUE.
        IF(LTOT.LT.0.0)DB(J)=.FALSE.
        DO 35 I=2,K
        D(I,1)=D(I,0)
35      CONTINUE
40      CONTINUE
```

CALCULATION OF PROB.OF ERROR

```
        NOE=0
        DO 50 I=1,LD
        IF(DB(I))GOTO 50
        NOE=NOE+1
50      CONTINUE
        TNE=NOE
        POE=TNE/LD
        WRITE(31,54)PWR,PES,K,LD
54      FORMAT(/1X,'OPT.POWER = ',E16.4,' EQ.RESISTANCE = ',E16.8,
     1  ' NO.OF USERS = ',T4,' DATA LENGTH = ',I7)
        WRITE(31,55)NOE,POE
55      FORMAT(//1X,'NO.OF ERRORS =',I5,'  PROB.OF ERROR = ',E16.8)
        CLOSE(UNIT=18,DEVICE='DSK')
        CLOSE(UNIT=30,DEVICE='DSK')
        CLOSE(UNIT=31,DEVICE='DSK')
        STOP
        END
```

SUBROUTINE TO FIND THE OTHER USERS' SIGNAL CONTRIBUTION
TO LAMDA(t)

```fortran
      SUBROUTINE MODSEQ(KS,TDS,DS,NS)
      INTEGER AS(25,0:511),BS(0:511),TDS(25),BM(25,0:511),TAU
      LOGICAL DS(25,0:1),DAT0,DAT1
      COMMON BM,AS,BS
      DO 5 IS=2,KS
      TAU=TDS(IS)
      DAT0=DS(IS,0);DAT1=DS(IS,1)
      IF(.NOT.DAT1)GOTO 20
      GOTO 30
20    DO 1 JS=0,TAU-1
      BM(IS,JS)=-AS(IS,NS-TAU+JS)
1     CONTINUE
      GOTO 40
30    DO 2 JS=0,TAU-1
      BM(IS,JS)=AS(IS,NS-TAU+JS)
2     CONTINUE
40    IF(.NOT.DAT0)GOTO 50
      GOTO 60
50    DO 3 JS=TAU,NS-1
      BM(IS,JS)=-AS(IS,JS-TAU)
3     CONTINUE
      GOTO 5
60    DO 4 JS=TAU,NS-1
      BM(IS,JS)=AS(IS,JS-TAU)
4     CONTINUE
5     CONTINUE
      DO 10 IS=0,NS-1
      ISUMS=0
      DO 9 JS=2,KS
      ISUMS=ISUMS+BM(JS,IS)
9     CONTINUE
      BS(IS)=ISUMS
10    CONTINUE
      RETURN
      END
```

EE-1984-M-RAO-SPR